

ORIGINAL RESEARCH

Novel and Highly Potent Therapeutic Agent, *Trametes Robiniophila* Murr (Huaier), Mitigates Pulmonary Vascular Remodeling in Rodents

Huangshu Ye , MD, PhD; Yue Zhang, MD, PhD; Li Hu , MD, PhD; Yuxin Feng, MD, PhD; Tianfan Zhu, MD; Qi Meng, MD; Xiaoxuan Sun, MD, PhD; Miaoja Zhang, MD, PhD; Zhengsheng Mao, MD, PhD; Feng Chen , MD, PhD; Yanfang Yu, MD; Qiang Wang, MD, PhD; Jie Wang , MD, PhD

BACKGROUND: Pulmonary hypertension (PH) is a critical disease causing right ventricular failure and early death. Conventional single-pathway treatments are inadequate, highlighting the need for new therapies. *Trametes robiniophila* Murr (Huaier), a traditional Chinese medicine, inhibits cancer cell proliferation. Importantly, the aberrant proliferation of pulmonary artery smooth muscle cells (PASMCs) is a key contributor to increased pulmonary vascular resistance in PH. However, it remains unknown whether Huaier could protect against PH. This study aimed to examine whether Huaier could protect against PH as well as its underlying mechanisms.

METHODS: Huaier treatment effectively mitigated hypoxia- and monocrotaline-induced PH in rodent models, as evidenced by reductions in pulmonary artery pressure, right ventricular hypertrophy, and vascular remodeling. Transcriptomic and network pharmacology analyses suggested that Huaier effectively alleviates PH primarily through inhibiting the phenotypic switching of PASMCs.

RESULTS: In vitro, Huaier suppressed PASMCs proliferation and migration in both PDGF (platelet-derived growth factor)-treated PASMCs and PH-PASMCs. Mechanistically, Huaier treatment was found to significantly inhibit the Hif1 α (hypoxia-inducible factor 1- α) signaling pathway, thereby reducing excessive lactate accumulation and abnormal glycolysis, and the NF- κ B (nuclear factor κ B) signaling pathway, thereby diminishing inflammatory responses. Additionally, Huaier activated the Nrf2 (nuclear factor erythroid 2-related factor 2) signaling pathway, enhancing mitochondrial function and alleviating oxidative stress. The multifunctional roles of Huaier contributed to its inhibited effect on PASMCs proliferation and thus improved vascular remodeling.

CONCLUSIONS: Huaier exerts multitarget therapeutic effects against PH by concurrently modulating metabolic reprogramming, inflammation and oxidative homeostasis, thereby inhibiting PASMCs-driven vascular remodeling. These findings position Huaier as a promising candidate for PH treatment, warranting further clinical trials to validate its translational potential.

Key Words: Huaier ■ multitarget therapy ■ pulmonary artery smooth muscle cells ■ pulmonary vascular remodeling

Correspondence to: Jie Wang, MD, PhD, Department of Forensic Medicine, Key Laboratory of Targeted Intervention of Cardiovascular Disease, Collaborative Innovation Center for Cardiovascular Disease Translational Medicine, Nanjing Medical University, 101 Longmian Avenue, Jiangning District, Nanjing, Jiangsu 210029, China. Email: wangjiefm@njmu.edu.cn; or Qiang Wang, MD, PhD, Department of Rheumatology, the First Affiliated Hospital of Nanjing Medical University, Nanjing, Jiangsu 210029, China, Email: jerrytortoise@163.com; or Yanfang Yu, M.D., Department of Forensic Medicine, Nanjing Medical University, Nanjing, Jiangsu 210029, China, Email: yanfangyu223@njmu.edu.cn

*H. Ye, Y. Zhang, and L. Hu contributed equally to this article.

This article was sent to Yen-Hung Lin, MD, PhD, Associate Editor, for review by expert referees, editorial decision, and final disposition.

Supplemental Material is available at <https://www.ahajournals.org/doi/suppl/10.1161/JAHA.125.041405>

For Sources of Funding and Disclosures, see page 22.

© 2025 The Author(s). Published on behalf of the American Heart Association, Inc., by Wiley. This is an open access article under the terms of the [Creative Commons Attribution-NonCommercial-NoDerivs](#) License, which permits use and distribution in any medium, provided the original work is properly cited, the use is non-commercial and no modifications or adaptations are made.

JAHA is available at: www.ahajournals.org/journal/jaha

RESEARCH PERSPECTIVE

What Is New?

- Huaier alleviates pulmonary hypertension in both hypoxia-induced mice and monocrotaline-induced rats, with improving hemodynamic parameters and reducing pulmonary vascular remodeling.
- This study provides strong evidence of a multimodal mechanism underlying the potent therapeutic effect of Huaier through its action in downregulating Hif1 α (hypoxia-inducible factor 1-alpha) to counteract glycolytic reprogramming, inhibiting NF- κ B (nuclear factor κ B) to prevent inflammation, and activating the Nrf2 (nuclear factor erythroid 2-related factor 2) antioxidant defense to alleviate oxidative stress; collectively, these mechanisms suppress pathological changes in pulmonary artery smooth muscle cells, highlighting Huaier's comprehensive approach against pulmonary hypertension.

What Question Should Be Addressed Next?

- Further research is necessary to isolate and characterize the bioactive constituents within Huaier extract that contribute to its antivasular remodeling effects.
- The potential impact of Huaier on other cell types, such as fibroblasts and immune cells, during the progression of pulmonary hypertension remains to be explored; future multicenter randomized controlled trials are essential to validate the clinical applicability of Huaier in the treatment of pulmonary hypertension.

Nonstandard Abbreviations and Acronyms

Hif1α	hypoxia-inducible factor 1-alpha
NF-κB	nuclear factor κ B
Nrf2	nuclear factor erythroid 2-related factor 2
PASMCs	pulmonary artery smooth muscle cells
PDGF	platelet-derived growth factor
PH	pulmonary hypertension
RVH	right ventricular hypertrophy

Pulmonary hypertension (PH) is a chronic, progressive disease marked by pathological pulmonary vascular remodeling, which leads to increased pulmonary vascular resistance and subsequent right ventricular hypertrophy (RVH), ultimately resulting in RV failure and premature mortality. It is generally estimated

that the global prevalence of PH is \approx 1% among the adult population, rising to 10% in individuals over the age of 65.¹ However, the current therapeutic options only partially improve symptoms and cannot reverse pulmonary vascular remodeling. Thus, the search for novel and highly potent therapeutic agents has become the primary focus in the field.

The pathogenesis of PH has not been fully elucidated. Many clinical conditions and diseases, including chronic obstructive pulmonary disease and connective tissue diseases, as well as pathological stimuli, such as hypoxia, oxidative damage, inflammatory cytokines, and growth factors, can induce the occurrence of pulmonary vascular remodeling. Pulmonary vascular remodeling is a complex pathological process characterized by the thickening of the intima, media, and adventitia layers of the distal pulmonary arteries (PAs). This process involves the abnormal proliferation and migration of PA smooth muscle cells (PASMCs), dysfunction of PA endothelial cells, dysregulation of the immune system, and in situ thrombosis, all of which contribute to the development of pulmonary vascular remodeling and PH. Among these factors, the aberrant proliferation of PASMCs is a key element in the development of pulmonary vascular remodeling. Additionally, intercellular communication mediated by the extracellular matrix, cytokines, and extracellular vesicles are also involved in the pathological progression of PH.² The current treatment approaches are dedicated to reverse above pathological conditions.

Despite notable advancements in PH treatment over the past 20 years, marked by the approval of several pharmacological agents such as endothelin receptor antagonists, phosphodiesterase-5 inhibitors, and prostaglandins, patient outcomes remain suboptimal. The current survival rates underscore this issue, with a 1-year survival rate of 85% and a 5-year survival rate of 53%.^{3,4} For several decades, therapeutic strategies for PH are urgently needed with antiproliferative effects on PASMCs. Nevertheless, the currently employed pharmacological agents in clinical practice for PH predominantly function as pulmonary vasodilators. These agents are capable of enhancing hemodynamics and improving quality of life, but their limited effectiveness in reversing the established pulmonary vascular remodeling and alleviating the persistent impairment of RV function is still observed. Previous research has shown that pharmacological interventions targeting a singular signaling pathway have not yielded the desired clinical outcomes in the treatment of PH. Hence, there is a critical need to develop and identify novel medications that exhibit alternative mechanisms of action to achieve greater efficacy.

Recent research has increasingly focused on natural products for pharmaceutical development, recognizing the natural bioactive components as a

valuable resource. Several natural compounds, such as curcuminol, formononetin, and resveratrol, have been demonstrated to have therapeutic potential for PH, attributed to their multitarget mechanisms, low toxicity, and minimal side effects.⁵ *Trametes robiniophila* Murr (Huaier), a medicinal mushroom derived from *T. robiniophila* Murr, contains effective medicinal ingredients.⁶ Currently, Huaier has received approval from the Chinese National Medical Products Administration and been demonstrated to have antitumor potential across various malignancies, including primary liver cancer, lung cancer, breast cancer, and gastrointestinal cancer.⁷ The principal bioactive constituents of Huaier have been identified as rutin, kaempferol, glucuronic acid, and genistein. Huaier demonstrates potential in suppressing cancer cell proliferation across various cancer types through inducing cell cycle arrest and apoptosis.⁸ Notably, the abnormal proliferation of PSMCs, resulting from dysregulated cell cycle and apoptotic resistance, is a critical factor in the pathogenesis of pulmonary vascular remodeling in PH. Therefore, we hypothesized that Huaier may possess the capability to inhibit PSMCs proliferation and improve pulmonary vascular remodeling and thus protect against PH.

In this study, we demonstrated for the first time that Huaier treatment ameliorates PH in experimental mouse and rat models. Mechanistic data revealed that Huaier inhibits the proliferation and migration of PSMCs through its antiglycolytic, anti-inflammatory, and antioxidant properties, primarily by inhibiting the Hif1 α (hypoxia-inducible factor 1- α) and NF- κ B (nuclear factor κ B) signaling pathways as well as activating Nrf2 (nuclear factor erythroid 2-related factor 2) signaling pathway. These findings suggest that Huaier represents a novel and highly potent therapeutic agent for the treatment of PH.

METHODS

The data that support the findings of this study are available from the corresponding author upon reasonable request.

Preparation of Huaier Extract

The electuary Huaier ointment used in this study was generously provided by Qidong Gaitianli Pharmaceutical Co., Ltd (Qidong, Jiangsu, China). The dissolution of Huaier extract was performed following established methodologies from previous studies.^{9,10} Briefly, the electuary ointment was dissolved in either a saline solution or DMEM and subsequently filtered through a 0.22 μ m filter to obtain a stock solution. This solution was stored at 4 °C for short-term use in both in vivo and in vitro experiments.

Animal Experiments

The experimental protocols involving animals were approved by the Animal Core Facility of Nanjing Medical University (IACUC-2206036, 2408061 and 2408062). This study used models of PH induced by chronic hypoxia in mice and monocrotaline in rats. All adult male C57BL/6 mice and Sprague–Dawley rats were sourced from the Animal Resource Center at Nanjing Medical University.

For the mice PH model, the mice were randomly assigned to 1 of 3 groups, each consisting of 8 mice: (1) the normoxia group, (2) the hypoxia group, and (3) the hypoxia group treated with Huaier extract (hypoxia+Huaier) group. The mice in the hypoxia group were placed in a hypoxia chamber with a controlled atmosphere of 10 \pm 0.5% O₂ and CO₂<0.5%, achieved by mixing room air with N₂, whereas the mice in the normoxia group were exposed to ambient air. On the 15th day, the hypoxia+Huaier group was administered a daily oral dose of 50 mg of Huaier extract via gavage, with the dosage determined based on previous studies.¹¹ The normoxia and hypoxia groups received an equivalent volume of saline solution using the same procedure. PH parameters were measured, and tissue samples were obtained on day 28 following hypoxia exposure.

For the rat PH model, the rats were assigned to 1 of 3 groups, each consisting of 8 rats: (1) the control group, (2) the monocrotaline group, and (3) the monocrotaline group treated with Huaier extract (monocrotaline+Huaier) group. The monocrotaline group was established through a single subcutaneous injection of monocrotaline at a dosage of 60 mg/kg. On the 15th day, the monocrotaline+Huaier group received a daily oral dose of 4.5 g/kg of Huaier extract via gavage. Throughout the experiment, all control groups were administered a corresponding volume of solvent. PH parameters were measured, and tissue samples were collected on the 28th day following the monocrotaline injection. No animals were excluded from analyses or outcome assessments in this study.

Transthoracic Echocardiography

Transthoracic echocardiography in rats was performed using the Vevo 2100 system (VisualSonics) equipped with a 30-MHz transducer probe. The rats were anesthetized with 5% isoflurane inhalation and maintained at 2% to 3% isoflurane during the examination. Then, the rats were placed supine on a homeothermic plate and shaved over the precordial region. PA acceleration time and ejection time were measured, and the ratio of PA acceleration time to PA ejection time was calculated as an indirect index of the PH.

Assessment of Right Ventricular Systolic Pressure and Right Ventricular Hypertrophy

In accordance with our prior descriptions, RV systolic pressure (RVSP) and RVH were measured.^{12,13} To summarize, a needle filled with heparinized saline was linked to a pressure transducer and inserted through the diaphragm into the RV. The RVSP was then recorded and measured with the PowerLab data acquisition system (AD Instruments) and LabChart 7.2 software. Next, the animals were euthanized and subjected to RVH measurements. The RV was separated from the left ventricle (LV) and septum to determine the weight and calculate the Fulton index (RV/LV + septum).

Assessment of Morphology and Histology

Following the assessment of hemodynamics, the pulmonary circulation was perfused with ice-cold PBS via the right ventricle, and major tissues, including the heart, liver, spleen, lungs, and kidneys, were collected for subsequent experimentation. The middle lobes of the right lung were fixed in 4% paraformaldehyde for 24 hours at 4°C, followed by dehydration in a 30% sucrose solution for 48 hours, and subsequently embedded in optimal cutting temperature compound. Cross-sections of 10 µm thickness were prepared using a freezing microtome (HM525 NX, Thermo Fisher) and stained with hematoxylin and eosin to visualize the wall thickness of small pulmonary vessels. Pulmonary vascular remodeling was evaluated by quantifying the degree of medial wall thickening in small pulmonary vessels with external diameters ranging from 25 to 100 µm. The extent of medial wall thickness was expressed as the ratio of medial area to cross-sectional area and analyzed using ImageJ software. To determine the level of muscularization, 40 to 60 small PAs (20–50 µm in diameter) were examined per mouse or rat, with muscularization expressed as the ratio of nonmuscular, partially muscular, and fully muscular vessels to the total number of vessels. All counts and measurements were conducted in a blinded manner.

Immunofluorescence Staining

The immunofluorescence staining procedure was conducted as follows: lung cryosections were allowed to air dry for 10 minutes at room temperature, followed by rehydration in PBS for 15 minutes at the same temperature. Cells cultured on glass coverslips were fixed with 4% paraformaldehyde in PBS for 15 minutes, and subsequently washed with PBS. Permeabilization of the samples was achieved using 0.3% Triton X-100/PBS for 15 minutes, followed by blocking with 3% BSA for 1 to 2 hours. The samples were then incubated with appropriate primary antibodies overnight at 4°C. Post

incubation, samples were washed twice with 0.1% Triton-PBS and incubated with suitable fluorescently labeled secondary antibodies for 1 to 2 hours in the dark at room temperature. All antibodies were diluted in a blocking buffer composed of PBS with 3% BSA. Subsequently, the samples were counterstained with DAPI to visualize nuclei and mounted using an anti-fluorescence quenching mounting medium. Imaging was conducted using a fluorescence microscope (Olympus, Tokyo, Japan), and fluorescence data were analyzed using ImageJ software. The antibodies used in this study are listed in Table S1.

TUNEL Staining

The One Step TUNEL Apoptosis Assay Kit (Beyotime, C1088) was used for TUNEL (terminal deoxynucleotidyl transferase-mediated dUTP-biotin nick end labeling) staining following instructions. Briefly, lung cryosections were fixed with 4% paraformaldehyde for 30 to 60 minutes, washed with PBS twice (10 minutes each), and permeabilized with 0.5% Triton X-100 in PBS for 5 minutes at room temperature. The sections were then incubated with 100 µL TUNEL reaction mixture at 37°C for 60 minutes. After washing with PBS, the nuclei were stained with DAPI, and the slides were mounted with an antifade mounting medium. Finally, the samples were observed under a fluorescence microscope.

Serum Biomarker Molecules of Liver and Kidney Functions

Blood samples were obtained via heart puncture at the time of euthanization and centrifuged to collect serum. Serum aspartate transaminase, alanine transaminase, total bilirubin, and creatinine levels were measured with an automatic biochemistry analyzer 7100 (Hitachi).

Cell Culture

Primary PSMCs were harvested from the PAs of rats and patients with PH, and then identified by immunofluorescence staining with α-SMA (alpha-smooth muscle actin) as previously described.^{14,15} All experiments involving PSMCs were conducted at passages 3 to 6, with cells serum starved for 12 hours before experimentation.

RNA-Sequencing

PAs were isolated from the left lobe of lung tissue in both the monocrotaline group (n=4) and the monocrotaline+Huaier group (n=4). Rat PSMCs (RPASMCs) were treated with or without Huaier (2 mg/mL) under PDGF (platelet-derived growth factor) conditions for 48 hours (n=4 for each group). Total RNA was extracted from PAs or RPASMCs using RNAiso

Plus (TaKaRa, #9109, Japan) in conjunction with chloroform. For RNA sequencing (RNA-seq), the RNA samples underwent sequencing by Lianchuan Biotech (Hangzhou, China) and were subsequently analyzed using the OmicStudio tools accessible at <https://www.omicstudio.cn/tool>. DESeq2 was used for statistical analysis of differential expression. Differentially expressed genes were defined as log2 fold changes >1 or <-1, with the Benjamini–Hochberg adjusted *P* values (false discovery rate) <0.05.

Network Pharmacology

The active small-molecule compounds of Huaier and their target genes were analyzed using the HERB database (<https://herb.ac.cn/>), a high-throughput experiment- and reference-guided database of traditional Chinese medicine. A total of 4 chemical compounds were extracted from the database. The GeneCards database (<https://www.genecards.org/>), OMIM diseases database (<https://omim.org/>) and Therapeutic Target Database (<https://db.idrblab.net/ttd/>) were used to gather the information of human target genes related to PH. Using the STRING database (<https://string-db.org/>), the protein–protein interaction network of the identified Huaier target genes in PH was analyzed and visualized using Cytoscape software (version 3.10.3).

The molecular structures of rutin, kaempferol, glucuronic acid, and genistein obtained from the PubChem database were brought into Chem3D for energy minimization and geometric optimization. The crystal structures of Hif1 α (PDB code: 4H6J), Nrf2 (PDB code: 2IZ1), and NF- κ B (PDB code: 1MY7) proteins were obtained from the PDB website. Molecular docking was simulated using AutoDock 1.5.7. It makes sense to calculate binding energies of <0 kcal/mol. PyMOL 2.6.0 software was used to map 3-dimensional chemical bonds and amino acid residues.

Cell Viability Assay

The viability of RPASMCs was determined using the Cell Counting Kit-8 (Beyotime, C0039) according to the manufacturer's instructions. The cells were seeded in 96-well plates and treated with different concentrations of Huaier extract. At the indicated time points, 10 μ L of Cell Counting Kit-8 solution diluted in 90 μ L DMEM were added in each well and the cultures were incubated at 37°C for 90 minutes. The optical density values were measured by a spectrophotometer at 450 nm.

Cell Cycle and Apoptosis Analysis

Cell apoptosis was detected with Annexin V-FITC/PI Apoptosis Detection Kit (Liankebio, AP101). Briefly, RPASMCs were seeded in 6-well plates and cultured overnight. The cells were subjected to various experimental conditions for 48 hours, with those incubated

in fresh culture medium serving as the control group. Subsequently, the cells were harvested, rinsed with PBS solution, and gently resuspended in 250 μ L of binding buffer. To this suspension, 5 μ L of Annexin V-FITC and 10 μ L of propidium iodide were added, followed by incubation in the dark for 5 minutes. A total of 10000 cells from each experimental group were analyzed using a FACS Calibur flow cytometer (BD Biosciences), and the data were processed with FlowJo software version 10.8.1. This procedure was replicated across at least 3 independent experiments.

Cell cycle analysis was conducted using the Cell Cycle and Apoptosis Analysis Kit (Beyotime, C1052) in accordance with the manufacturer's instructions. RPASMCs from the various treatment groups were fixed with cold 70% ethanol at 4°C overnight. The fixed cells were then collected and resuspended in PBS containing propidium iodide and RNase A, followed by incubation at room temperature in the dark for 30 minutes. DNA content was quantified using a FACS Calibur flow cytometer, and the distribution of cells across different cell cycle phases was determined using ModFit software version 5.0.

Cell Proliferation and Wound Healing Assay

Cell proliferation was detected using a Cell-Light EdU Apollo567 In Vitro Kit (RiboBio, C10310-1) according to the manufacturer's instructions. Cells were incubated with 10 μ M EdU for 4 hours before fixation with 4% paraformaldehyde. After permeabilization with 0.5% Triton X-100, the cells were stained with Apollo567 and DAPI. Images were taken with an Olympus fluorescence microscope and further analyzed using ImageJ software.

Cell migration capacity was measured by wound healing assay. PASMCS were seeded into 6-well plates cultured with different treatment and a line wound was scratched by a 1 mL pipette tip. The wounds were observed at 0, 6, 12, and 24 hours with a microscope. Finally, the width of scratches was measured and migration distance was calculated by ImageJ. Wound healing rate was computed using the formula: Wound healing rate = [(wound width at 0 hours) – (wound width at each time point)] / (wound width at 0 hours) × 100%.

DNA Damage Assessment by Comet Assay

DNA damage was evaluated using the Comet Assay Kit (Beyotime, C2041M). Initially, agarose-coated slides were prepared by embedding cells at a concentration of 1 × 10⁴ cells/mL in 0.7% low melting point agarose. These slides were then immersed in a lysis solution for 12 hours at 4°C. Subsequently, the slides were carefully removed and submerged in a rinse solution (comprising 1 mM EDTA, 200 mM NaOH, pH ~13) at room temperature for 20 to 60 minutes. Electrophoresis was

performed in the same solution for 20 to 30 minutes at a voltage of 0.75 to 1 V/cm. Finally, the slides were neutralized and stained with propidium iodide for 10 to 20 minutes, followed by observation under a fluorescence microscope. The percentage of Tail DNA was calculated to determine the Tail/Head DNA ratio for individual cells using ImageJ software.

Intracellular Reactive Oxygen Species, L-Lactate, Superoxide Dismutase, Glutathione Peroxidase-Px, Glutathione, and Malondialdehyde Assays

The intracellular reactive oxygen species (ROS) levels were assessed using a ROS detection kit (Beyotime, S0033S). A concentration of 10 μ M DCFH-DA was added to each well of the culture plate, followed by a 30-minute incubation period in the dark. Imaging was conducted using the EVOS™ XL inverted microscope. The levels of L-lactate (Beyotime, S0208S), SOD (superoxide dismutase; Beyotime, S0101S), total GSH-Px (glutathione peroxidase; Beyotime, S0059S), total GSH (glutathione; Beyotime, S0052) and malondialdehyde (Beyotime, S0131S) in RPASMCs were estimated according to the manufacturer's instructions.

Mitochondrial Imaging

Mitochondria were stained by Mito-Tracker Red CMXRos (Beyotime, C1035) according to the manufacturer's instructions. Mitochondrial images were obtained by an Olympus fluorescence microscope and the mitochondrial network morphology was analyzed by FIJI with Mina plug-in.

RNA Extraction and Quantitative Real-Time Polymerase Chain Reaction

Total RNA was extracted from cultured RPASMCs using TriZol reagent (TaKaRa, #9109, Japan) according to the manufacturer's protocol. RNAs were quantified using a NanoDrop 2000 instrument (ThermoFisher) and converted to cDNA by reverse transcription using the TransScript One-Step gDNA Removal and cDNA Synthesis SuperMix Kit (abm, G592). Quantitative polymerase chain reaction was performed using the Blastq Green 2X qPCR MasterMix (abm, G891) on a Quantagene q225 real-time polymerase chain reaction system (Kubo, China). For relative quantification of target gene mRNA expression, normalization was performed against β -actin expression using the comparative $2^{-\Delta\Delta Ct}$ method. The primers used in this study are listed in Table S2.

Western Blotting

Western blotting was performed as previously described.¹⁶ Briefly, total proteins in tissues or cells were

extracted in ice-cold RIPA (Beyotime, P0013C) buffer containing pierce protease inhibitors (Thermo Fisher Scientific, A32953) and PMSF (Beyotime, ST507). Protein concentration was measured using the BCA Protein Assay Kit (Beyotime, P0011). Samples were combined with 5 \times SDS loading buffer, subjected to boiling for 8 minutes, and then resolved on 8% to 12% SDS-polyacrylamide gels. Subsequently, proteins were transferred onto a PVDF membrane (Millipore). The membranes were blocked with either 5% nonfat milk or 3% BSA solution TBS containing 0.1% Tween 20 for 1 to 2 hours, followed by an overnight incubation with primary antibodies at 4°C. The following day, membranes were washed three times with TBS containing 0.1% Tween-20 for 10 minutes each and incubated with horseradish peroxidase-conjugated secondary antibodies for 1 hour at room temperature. Finally, protein bands were visualized using a chemiluminescence detection system (Tanon), and relative protein levels were quantified through ImageJ densitometry analysis. The antibodies used in this study are listed in Table S1.

Statistical Analysis

Statistical analyses were conducted using Prism 9.0 (GraphPad Software). Data are expressed as the mean \pm SE, with in vitro experiments conducted and analyzed across a minimum of 3 independent replicates. To compare the means between 2 groups, the Levene's test was employed to assess the homogeneity of variance. An unpaired 2-sided Student's *t* test was used when equal variance was confirmed; otherwise, Welch's *t* test assuming unequal variance was applied. For comparisons involving >2 groups, the Brown-Forsythe test was used to evaluate variance homogeneity. If equal variance was observed, a 1-way ANOVA was conducted, followed by a post hoc analysis using the Bonferroni method to adjust for multiple comparisons. In cases of unequal variance, a Welch ANOVA was performed, followed by a post hoc analysis using the Tamhane T2 method. Correlation analyses between PA transcripts and RVSP and right ventricle/(LV+septum) were performed using Pearson's correlation coefficient. Statistical significance was defined as *P*<0.05. Randomization and blinded analyses were implemented wherever possible.

RESULTS

Huaier Alleviated Pulmonary Vascular Remodeling in Experimental Rodent PH Models

To assess the effects of Huaier on PH in vivo, we initially established a hypoxia induced PH mouse model. Mice were exposed to hypoxia, and oral administration

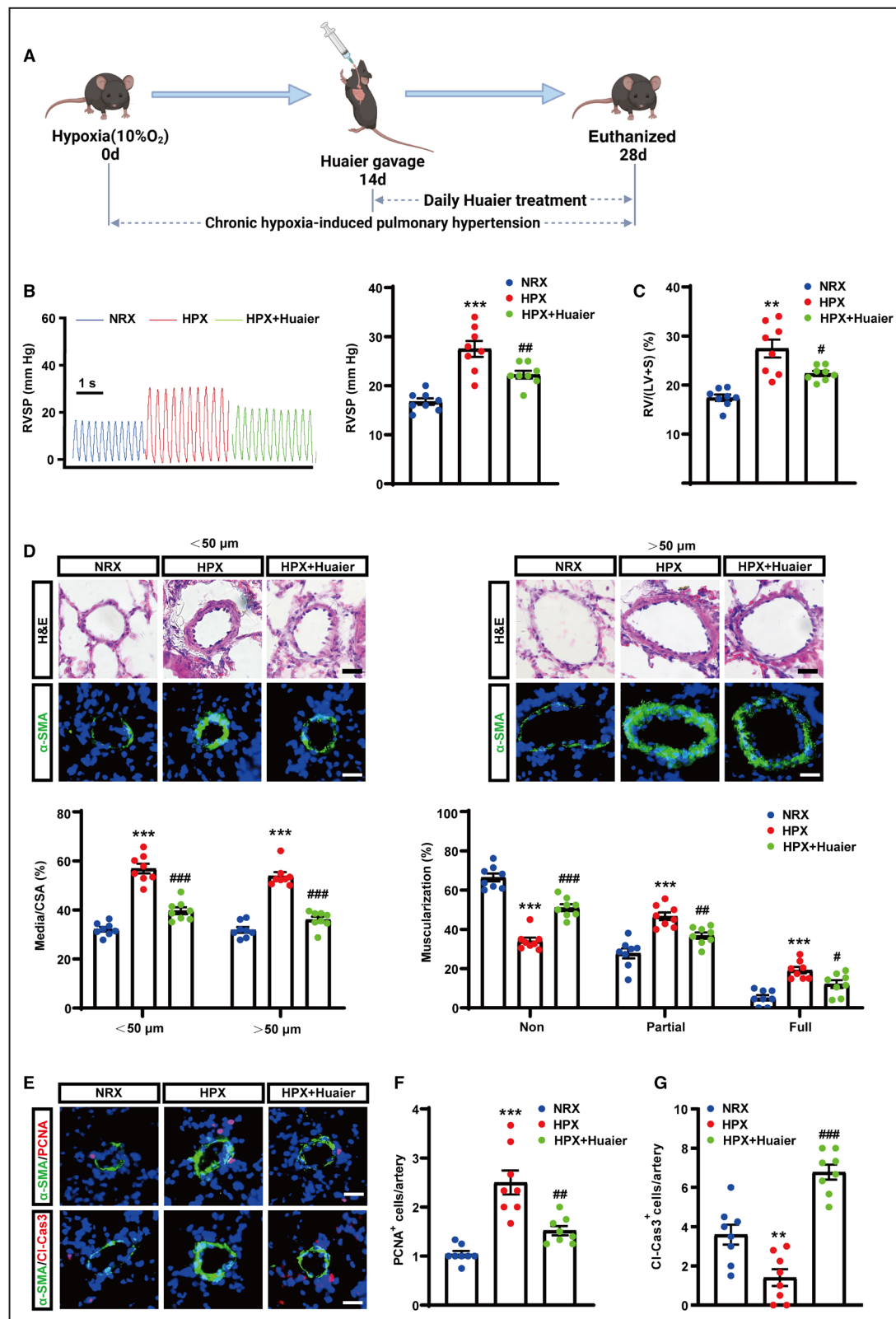
of Huaier began 2 weeks after this exposure. Treatment was administered daily for 14 consecutive days, and the mice were euthanized at 28 days (Figure 1A). The RVSP and right ventricle/(LV+septum) were significantly increased in the hypoxia group compared with the normoxia group, confirming the successful establishment of PH animal model. After 14 days of oral Huaier administration, there was a marked reduction in RVSP and RVH compared with the hypoxia group (Figure 1B and 1C). Subsequently, pulmonary vascular remodeling was evaluated by measuring the wall thickness ratio and muscularization. Hematoxylin and eosin and immunofluorescence staining revealed that the small PAs in the hypoxia group exhibited thicker vessel walls, whereas Huaier treatment mitigated these pathological changes in the lungs. Furthermore, Huaier significantly reduced the muscularization of PAs in hypoxia-induced PH mice (Figure 1D). Additionally, the SMC proliferation observed in the hypoxia group was diminished in mice treated with Huaier, as indicated by the number of PCNA (proliferating cell nuclear antigen) positive cells per PA (Figure 1E and 1F). Tissue TUNEL staining and immunofluorescence analysis of cleaved caspase 3 indicated a near absence of apoptotic cells surrounding the thickened vasculature in the PAs of the hypoxia group. Conversely, Huaier-treated mice exhibited an increase in TUNEL- and cleaved caspase-3-positive cells compared with the hypoxia group (Figure 1E through G; Figure S1A). Histopathological analysis indicated that no clear or readily detectable pathological changes were observed in the major organs of hypoxia-induced PH mice following Huaier treatment (Figure S1B). These results indicated that Huaier could ameliorate hypoxia-induced PH in mice without leading to observable side effects.

The monocrotaline-induced rat PH model is frequently used to study a severe condition of PH. To further substantiate the therapeutic effects of Huaier on severe pathological pulmonary vascular remodeling following the onset of PH, we next employed the monocrotaline-induced rat PH model (Figure S2A). Our findings indicated that rats administered monocrotaline exhibited reduced weight gain, attributed to decreased activity and foraging behavior. Conversely, rats receiving Huaier treatment demonstrated significant mitigation of these conditions, evidenced by a notable increase in weight gain compared with the monocrotaline group (Figure S2B). The administration of monocrotaline occasionally leads to animal fatality due to significant advance of pulmonary vascular remodeling and heart failure. We found that 2 rats in the monocrotaline group succumbed post model establishment; notably, there were no fatalities in the Huaier treatment group (Figure S2C). These results suggest that Huaier extract significantly enhanced the quality of life and survival

in the monocrotaline-induced rat PH model. As anticipated, Huaier significantly attenuated the elevated RVSP and RV hypertrophy compared with monocrotaline treatment alone (Figure 2A and 2B). Additionally, it also improved the PA acceleration time/PA ejection time, as measured by echocardiography (Figure 2C). Histological analysis demonstrated that Huaier reduced pulmonary vascular remodeling and decreased the percentage of PCNA-positive cells in small PAs in the monocrotaline-induced rat PH model (Figure 2D through E). A significant increase in cleaved caspase-3-positive and TUNEL-positive vascular cells was also observed in the PAs of the monocrotaline+Huaier group compared with the monocrotaline group (Figure 2E through G; Figure S2D). Furthermore, histopathological analysis revealed no significant pathological lesions in the major organs of monocrotaline-induced PH rats following Huaier treatment (Figure S3A). Additionally, serum biochemical parameters reflecting liver and kidney function were assessed. Apart from a reduction in total bilirubin levels in the Huaier treatment group, no significant differences were observed in aspartate transaminase, alanine transaminase, and creatinine levels between the monocrotaline and monocrotaline+Huaier groups (Figure S3B). These findings indicate that Huaier effectively mitigated pulmonary vascular remodeling and enhanced RV function in the monocrotaline-induced PH model without observable side effects, suggesting favorable drug safety while treating PH.

Huaier Targets PSMCs to Mitigate Pulmonary Vascular Remodeling

To determine the reason that Huaier alleviates PH, we further found that there was a significant upregulation of the cell cycle inhibitor P27 and a downregulation of proliferation markers cyclin D1 (Cnd1) and PcnA in the PAs of monocrotaline-induced PH rats treated with Huaier (Figure 3A). To further elucidate the mechanisms underlying the beneficial effects of Huaier on PH, RNA-seq was performed in the PAs of rats from both the monocrotaline group and the monocrotaline+Huaier treatment group. Heatmap and hierarchical clustering analyses of the RNA-seq data revealed a clear distinction between the monocrotaline and monocrotaline+Huaier groups (Figure 3B). Our analysis identified 66 differentially expressed genes ($|\log_2FC| > 1$ with false discovery rate adjusted P value < 0.05) in the PAs of monocrotaline-induced rats treated with Huaier extract compared with those treated with monocrotaline alone (Figure S4A). To evaluate functional enrichment, we performed a Kyoto Encyclopedia of Genes and Genomes pathway analysis using gene set enrichment analysis (GSEA). The GSEA of the biological functions indicated significant



upregulated enrichment in pathways pertinent to the cytoskeleton in muscle cells, vascular smooth muscle contraction, and mitochondrial electron transport (NADH to ubiquinone) (Figure 3C and 3D).

Using the HERB database, we identified 4 active components in Huaier: genistein, glucuronic acid, kaempferol, and rutin. In order to understand the bioactive components of Huaier and the effect on their target

Figure 1. Huaier extract alleviates chronic hypoxia-induced PH in mice.

A, Schematic representation of Huaier extract treatment in hypoxia-induced PH mouse model. **B**, Representative images and quantification of the RVSP in normoxia, hypoxia and hypoxia+Huaier groups. **C**, The weight ratio of RV/(LV+S) in each group. **D**, Representative images of H&E staining and α -SMA (green) immunofluorescence staining of the pulmonary vascular vessels, and quantification of vascular medial thickness as well as the proportion of non-, partially, or fully muscularized PAs. **E**, Representative images of immunofluorescence staining of lung tissues for α -SMA (green) and PCNA (red), as well as α -SMA (green) and CI-Cas3 (red) were shown. **F**, The number of PCNA-positive cells was quantified in each of the PAs. **G**, Quantitative analysis of the number of CI-Cas3-positive cells in pulmonary vascular vessels. $n=8$ mice per group. Data are presented as mean \pm SE; P values were determined by 1-way ANOVA with Bonferroni post hoc test (**B**, **D**, and **G**) and Welch ANOVA with Tamhane T2 post hoc test (**C** and **F**). ** $P<0.01$ and *** $P<0.001$ vs normoxia group; # $P<0.05$, ## $P<0.01$ and ### $P<0.001$ vs hypoxia group. Scale bars=20 μ m. CI-Cas3 indicates cleaved caspase-3; CSA, cross-sectional area; H&E, hematoxylin and eosin; HPX, hypoxia; NRX, normoxia; PAs, pulmonary arteries; PCNA, proliferating cell nuclear antigen; PH, pulmonary hypertension; RV/(LV+S), the ratio of right ventricle to left ventricle wall plus septum; RVSP, right ventricular systolic pressure; and α -SMA, α -smooth muscle actin.

genes, we subsequently investigated the genes affected by these small-molecule compounds and 147 genes were identified, enabling the construction of a component-target network (Figure S4B). Further cross-referencing these with 1142 PH-related genes from GeneCards, OMIM, and Therapeutic Target Databases identified 70 overlapping genes as potential Huaier targets in PH (Figure 3E). Additionally, the protein-protein interaction network analysis revealed complex interactions among these genes and further demonstrated that the key targets of Huaier against PH are primarily associated with inflammatory factors and Hif1 α (Figure S4C). The results of the biological process functional enrichment analysis showed that these genes were significantly enriched in the regulation of SMC proliferation and cellular response to oxidative stress (Figure 3F). These data suggested that Huaier may improve pulmonary vascular remodeling by targeting proliferating SMCs.

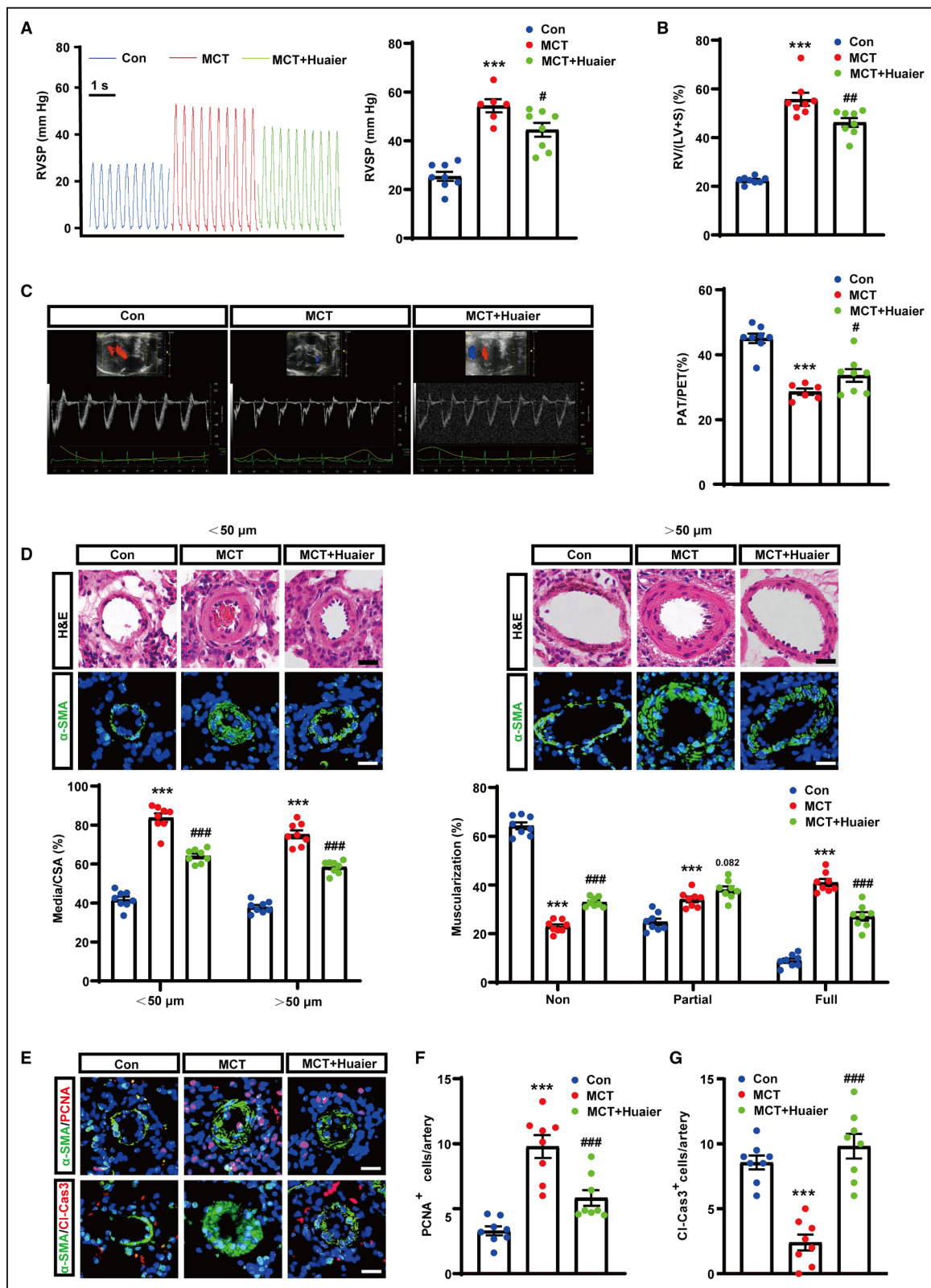
Huaier Suppressed Classical Complement Activation and Cytokine Signaling

A growing body of preclinical and clinical research on PH has highlighted the critical role of inflammation in the pathogenesis of the disease.¹⁷ Elevated levels of various cytokines and chemokines have been observed in both animal models of PH and human patients. Notably, the extent of perivascular inflammation in PH correlates with pulmonary hemodynamics, vascular alterations, and clinical outcomes.^{18,19} Hence, we investigated how Huaier affected the inflammatory/cytokine signaling pathway in our RNA-seq data of PAs. GSEA of Kyoto Encyclopedia of Genes and Genomes and Gene Ontology pathways revealed that the cytokine-cytokine receptor interaction, chemokine signaling pathway, and complement and coagulation cascade were downregulated after Huaier treatment in monocrotaline-induced PH rat PAs (Figure S5A–C). Correlation heatmaps further demonstrated that the expression levels of several transcripts within the cytokine and chemokine pathways were associated with RVSP and RVH (Figure S5D). Given

that the complement system facilitates cytokine and chemokine release,²⁰ we assessed the transcript levels related to the complement/coagulation pathway. Correlation analysis revealed a significant association between C2, C3, C9, and *Igll1* with both RVSP and right ventricle/(LV+septum) (Figure S5E). These findings suggest that Huaier may downregulate the expression of genes related to the complement system and reduce the levels of proinflammatory cytokines and chemokines, potentially mitigating the inflammatory response in PH.

Huaier Inhibited the Proliferation, Migration and Phenotypic Switching of PSMCs

The phenotypic switching of PSMCs is critical in the progression of pulmonary vascular remodeling during PH development.^{3,21} To investigate the mechanisms underlying the potential beneficial effects of Huaier on PH, we next focused on the in vitro analysis of PSMCs. Huaier inhibited the activity of RPASMCs in the presence of PDGF, with an inhibitory concentration 50 of 7.559 mg/mL (Figure S6A). Based on this inhibitory concentration 50 value, concentrations of 1, 2, 4, and 6 mg/mL of Huaier were employed in further experimental analysis. Cell Counting Kit-8 assays indicated that RPASMCs proliferation was increased in the PDGF group and diminished by Huaier treatment (Figure 4A). To examine the regulatory effects of Huaier on the proliferation and migration of RPASMCs, we exposed these cells to Huaier at concentrations of 1, 2, 4, and 6 mg/mL in the presence of PDGF. Our findings indicated that PDGF significantly enhanced the proliferation and migration of RPASMCs, whereas Huaier treatment markedly inhibited proliferation and significantly delayed wound closure in a concentration-dependent manner (Figure 4B through D). Given that cell proliferation is governed by cell cycle regulation, cell cycle analysis demonstrated that Huaier induced cell cycle arrest at the G2 phase (Figure 4E through F). Furthermore, annexin V-FITC and propidium iodide double-staining assays, conducted via flow cytometry,



were employed to assess apoptosis rates following 48 hours of exposure to Huaier extract. The results showed that both early and late apoptosis rates were increased in a concentration-dependent manner in

RPASMCs (Figure 4F through G). Western blot analysis revealed that PDGF increased the proteins levels of Pcn and Ccnd1 while reducing P27 protein expression in RPASMCs, whereas Huaier treatment effectively

Figure 2. Huaier extract alleviates monocrotaline-induced PH in rats.

A, Representative images and quantification of the RVSP in Con, monocrotaline, and monocrotaline+Huaier groups. **B**, The weight ratio of RV/(LV+S) in each group. **C**, Representative images of echocardiography showing parasternal short-axis views and pulsed-wave Doppler traces from the RV outflow tract in rats and quantification of PAT/PET. **D**, Representative images of H&E staining and α -SMA (green) immunofluorescence staining of the pulmonary vascular vessels, and quantification of vascular medial thickness and proportion of non-, partially, or fully muscularized PAs. **E**, Representative images of immunofluorescence staining of lung tissues for α -SMA (green) and PCNA (red), as well as α -SMA (green) and Cl-Cas3 (red) were shown. **F**, The number of PCNA-positive cells was quantified in each PAs. **G**, Quantitative analysis of the number of Cl-Cas3-positive cells in pulmonary vascular vessels. $n=6-8$ rats per group. The data are presented as mean \pm SE; P values were determined by 1-way ANOVA with Bonferroni post hoc test (**A-D**, **F-G**) and Welch ANOVA with Tamhane T2 post hoc test (**D**, for proportion of nonmuscularized PAs). *** $P<0.001$ vs Con group; # $P<0.05$, ## $P<0.01$ and ### $P<0.001$ vs monocrotaline group. Scale bars=20 μ m. Cl-Cas3 indicates cleaved caspase-3; Con, control; CSA, cross-sectional area; H&E, hematoxylin and eosin; MCT, monocrotaline; PAs, pulmonary arteries; PAT/PET, pulmonary artery acceleration time/pulmonary artery ejection time; PCNA, proliferating cell nuclear antigen; PH, pulmonary hypertension; RV/(LV+S), the ratio of right ventricle to left ventricle wall plus septum; RVSP, right ventricular systolic pressure; and α -SMA, α -smooth muscle actin.

reversed these alterations (Figure 4H). In addition, Huaier was also found to inhibit both proliferation and migration of human PSMCs treated with PDGF (Figure S7), as well as PH-PSMCs (Figure S8).

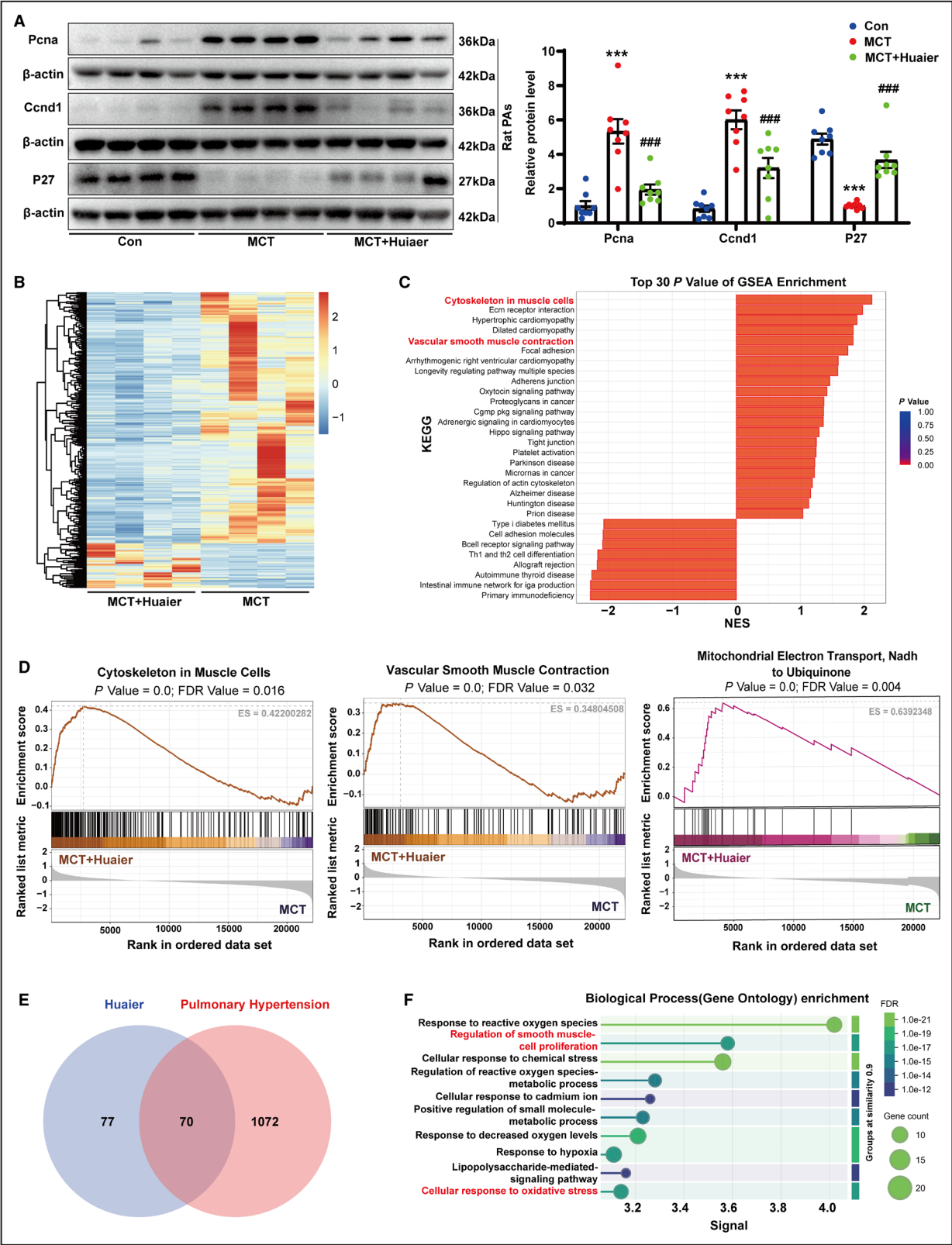
Huaier Suppressed Glycolysis by Inhibiting the Hif1 α Signaling Pathway in PSMCs

To elucidate the molecular mechanisms underlying the effects of Huaier extract on PSMCs in the pathogenesis of PH, we performed RNA-seq analysis to identify potential targets of Huaier. We prepared samples of RPASMCs treated with PDGF alone and PDGF+Huaier, and subjected them to transcriptome sequencing analysis. A total of 1850 genes exhibited differential expression patterns, with changes >2-fold and an adjusted P value of <0.05 (Figure S9A). Hierarchical clustering was used to delineate the distinct RNA profiles between the 2 groups (Figure S9B). The top 30 GSEA results, ranked by enrichment score, are shown in Figure S9C. These results primarily indicated enrichment in pathways related to glycolysis, cytokine activity, and immune response, which play critical regulatory roles in the proliferation and migration of PSMCs. According to the RNA-seq data, genes associated with cell differentiation were upregulated, whereas those involved in the positive regulation of cell migration, cell population proliferation, and several receptor-related genes were downregulated (Figure S9D-F). Furthermore, both GSEA and heatmap analyses revealed significant downregulation of genes involved in the Hif signaling pathway and glycolysis in RPASMCs treated with Huaier (Figure 5A and 5B; Figure S9G). PSMCs demonstrate enhanced proliferation under PH conditions, relying heavily on glycolysis to sustain their elevated proliferation rates. Hif1 α plays a crucial role in regulating glycolytic metabolism.²² Lactate, the end product of glycolysis, serves as a biomarker for glycolytic activity. Consequently, we quantified the levels of L-lactate in RPASMCs treated with Huaier at concentrations of 1 mg/mL and 4 mg/mL. The findings indicated that Huaier reduced lactate levels in a dose-dependent

manner (Figure 5C). Western blot analysis further revealed that PDGF upregulated the expression of Hif1 α and several glycolytic enzymes, including Pfkfb3 (6-phosphofructo-2-kinase/fructose-2,6-bisphosphatase 3). Conversely, Huaier treatment mitigated these effects (Figure 5D; Figure S10A). Additionally, quantitative real-time polymerase chain reaction results demonstrated that Huaier significantly downregulated the expression of various glycolytic genes (Figure 5E). Molecular docking studies suggested that the bioactive constituents of Huaier (rutin, kaempferol, glucuronic acid, and genistein) could directly bind to Hif1 α (Figure 5F). These findings indicate that Huaier plays a potential role in the treatment of PH by inhibiting the Hif1 α signaling pathway.

Huaier Improved Oxidative Stress by Activating Nrf2 Signaling Pathway in PSMCs

Oxidative stress, a characteristic feature of PH, exerts a substantial impact on pulmonary vascular remodeling by promoting cellular proliferation and migration.²³ The GSH metabolic pathway functions as a crucial defense mechanism against oxidative stress. In RPASMCs treated with Huaier, transcriptomic analysis revealed a significant upregulation of the GSH metabolic pathway (Figure 6A). The Nrf2 signaling pathway is pivotal in mediating cellular defense against oxidative stress. A heatmap was constructed to illustrate the elevated transcription levels of Nrf2 target genes in the Huaier-treated group (Figure 6B). Consequently, we further investigated the effects and regulatory mechanisms of Huaier in the context of PDGF-induced oxidative stress in RPASMCs. Huaier treatment led to a significant decrease in Keap1 (Kelch-like ECH-associated protein 1) levels, a known suppressor of Nrf2. Furthermore, Huaier enhanced the expression of Nrf2 and its downstream targets, Hmox1 (heme oxygenase 1) and Gpx4 (glutathione peroxidase 4), in RPASMCs (Figure 6C; Figure S11A). The activation of the Nrf2 pathway was further confirmed by immunofluorescence staining, indicating a pronounced activation of this pathway (Figure 6D).



Concurrently, Huaier effectively inhibited the excessive production of ROS induced by PDGF (Figure 6E). We assessed SOD activity, GSH-Px enzyme activity, GSH levels, and malondialdehyde levels in RPASMCs. The findings

demonstrated that Huaier significantly upregulated the expression of antioxidant enzymes (SOD, GSH-Px, and GSH) and reduced the expression of the PDGF-induced lipid peroxidation product (malondialdehyde) (Figure 6F).

Figure 3. Huaier extract mitigates pulmonary vascular remodeling through the suppression of PSMCs proliferation, as evidenced by RNA sequencing analysis of PAs.

A, Representative immunoblots and relative densitometric analysis of PcnA, Ccnd1, and P27 protein expression in PAs; β -actin was used to verify equivalent loading ($n=8$). **B**, Heatmap representing the differential gene expression patterns of PAs between Huaier extract treated group and untreated group ($n=4$). **C**, The top 30 KEGG pathways enriched were performed by GSEA based on RNA sequencing profiles. **D**, GSEA enrichment plots based on RNA sequencing profiles of PAs show that Huaier extract treatment results in the upregulation of the cytoskeleton in muscle cells pathway, the vascular smooth muscle contraction pathway, and the mitochondrial electron transport (NADH to ubiquinone) pathway. **E**, Venn diagram of the identified Huaier-targeted genes in PH shows 70 potential target genes. **F**, Biological process functional enrichment analysis of the identified Huaier-targeted genes in PH by GO analysis. The data are presented as mean \pm SE; P values were determined by 1-way ANOVA with Bonferroni post hoc test (**A**). *** $P<0.001$ vs Con group; ### $P<0.001$ vs monocrotaline group. Ccnd1 indicates CyclinD1; Con, control; FDR, false discovery rate; GO, Gene Ontology; GSEA, gene set enrichment analysis; KEGG, Kyoto Encyclopedia of Genes and Genomes; MCT, monocrotaline; NES, normalized enrichment score; PAs, pulmonary arteries; PSMCs, pulmonary artery smooth muscle cells; PCNA, proliferating cell nuclear antigen; and PH, pulmonary hypertension.

Oxidative stress is directly linked to mitochondrial dysfunction. By using MitoTracker, we found that Huaier treatment could increase mitochondrial networks (Figure S11B). Molecular docking simulations of Huaier's small molecule compounds with Nrf2 revealed binding energies of -7.8 , -6.4 , -5.0 , and -6.3 kcal/mol, suggesting spontaneous binding interactions (Figure S11C). Collectively, these findings suggest that Huaier alleviates oxidative stress induced by PDGF in RPASMCs.

Huaier Inhibited the NF- κ B Pathway and Relieved Inflammation in PSMCs

The NF- κ B pathway is integral to the processes of dedifferentiation, proliferation, and migration of PSMCs.^{24,25} Transcriptome GSEA of PAs from monocrotaline-induced rats and PDGF-treated PSMCs demonstrated a downregulation of the NF- κ B pathway following Huaier treatment (Figure S12A; Figure 7A). This finding was corroborated by Western blot analysis, which indicated that Huaier inhibited both the phosphorylation and nuclear translocation of p65 in PDGF-treated PSMCs (Figure 7B and 7C; Figure S13A). Additionally, our research suggests that Huaier may modulate the NF- κ B pathway by suppressing IKK (inhibitor of κ B kinase) phosphorylation (Figure S12B). Furthermore, heatmap analysis revealed that Huaier extract downregulated the transcription of proinflammatory genes (Figure S14A). The anti-inflammatory properties of Huaier were substantiated through the quantification of proinflammatory mediators (Figure 7E; Figure S14B). Molecular docking studies revealed that the 4 compounds present in Huaier exhibited strong binding affinity with the target protein, with binding energies of <-5 kcal/mol (Figure 7D). Altogether, these findings imply that Huaier modulates the NF- κ B pathway and mitigates inflammation.

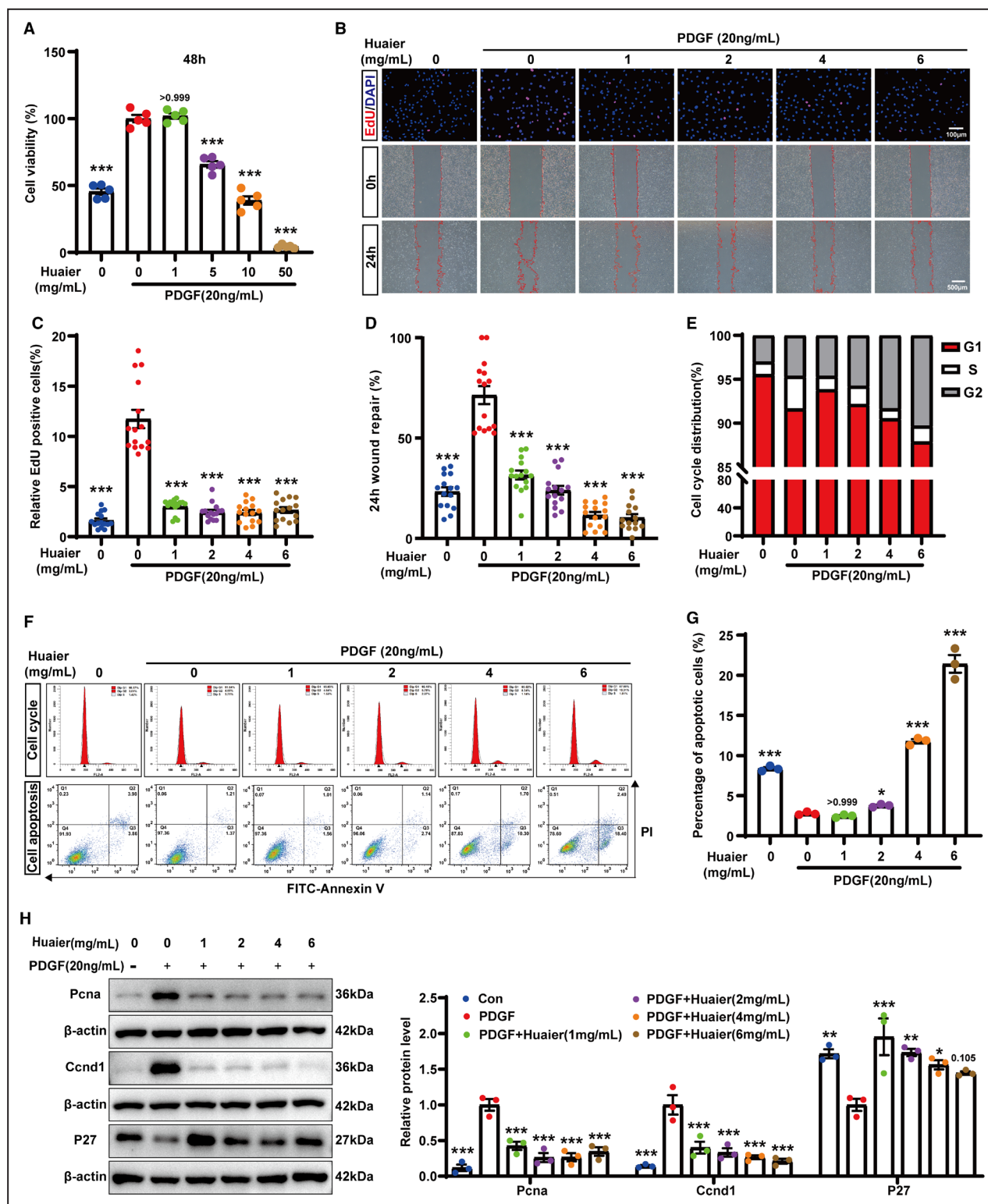
Huaier Inhibited DNA Damage in RPASMCs

Recent evidence highlights the role of impaired DNA damage response mechanisms in conferring

resistance to apoptosis and promoting a proliferative phenotype in PH-PASMCs.²⁶ Our observations indicate that Huaier treatment significantly reduced the protein levels of γ -H2ax and decreased the pRPA32/RPA32 (phospho-replication protein A 32/replication protein A 32) ratio in PDGF-induced PSMCs (Figure S15A). Furthermore, the fluorescence intensity of γ -H2ax was diminished in PDGF-stimulated RPASMCs following Huaier treatment, compared with untreated PDGF-stimulated RPASMCs (Figure S15B). The comet assay revealed PDGF-induced comet formation in RPASMCs, whereas Huaier treatment resulted in a significant reduction in tail length across (Figure S15C). These data suggest that Huaier effectively mitigates the DNA damage burden. PH is characterized by elevated levels of inflammatory cytokines, such as TNF- α (tumor necrosis factor alpha), IL-6 (interleukin-6), and PDGF, which promote DNA damage, as well as oxidative stress that induces DNA damage through base oxidation and deamination.²⁷ Therefore, the anti-inflammatory and antioxidant properties of Huaier may attenuate PDGF-induced DNA damage in RPASMCs.

DISCUSSION

At present, the majority of pharmacological interventions for PH employed in clinical settings are single-target treatments with limited effect in improving symptoms but not able to reverse pulmonary vascular remodeling. In accordance with the traditional paradigm of "1 disease, 1 target, 1 therapeutic agent," the inhibition of a single disease pathway may prompt the body to activate alternative related pathways to preserve disease homeostasis. Consequently, for diseases like PH, which are characterized by complex causes, single-target drugs often struggle to effectively disrupt the disease's comprehensive regulatory network. Traditional Chinese Medicine (TCM) has emerged as a prominent area of research within the domain of PH therapeutics, primarily due to its unique advantages in multicomponent synergy and multitarget regulation. Its pharmacological properties, characterized by low



toxicity, minimal side effects, and cost-effectiveness, align well with the requirements for the long-term management of chronic cardiopulmonary diseases.⁵ However, the integration of TCM into mainstream PH management presents both challenging and promising future directions.

Recent studies have provided substantial evidence supporting the appropriateness of TCM and natural products for treating PH across various animal models. For instance, research conducted by Wang et al. demonstrated that Dan-Shen-Yin granules could prevent the progression of PH in a hypoxia-induced mouse

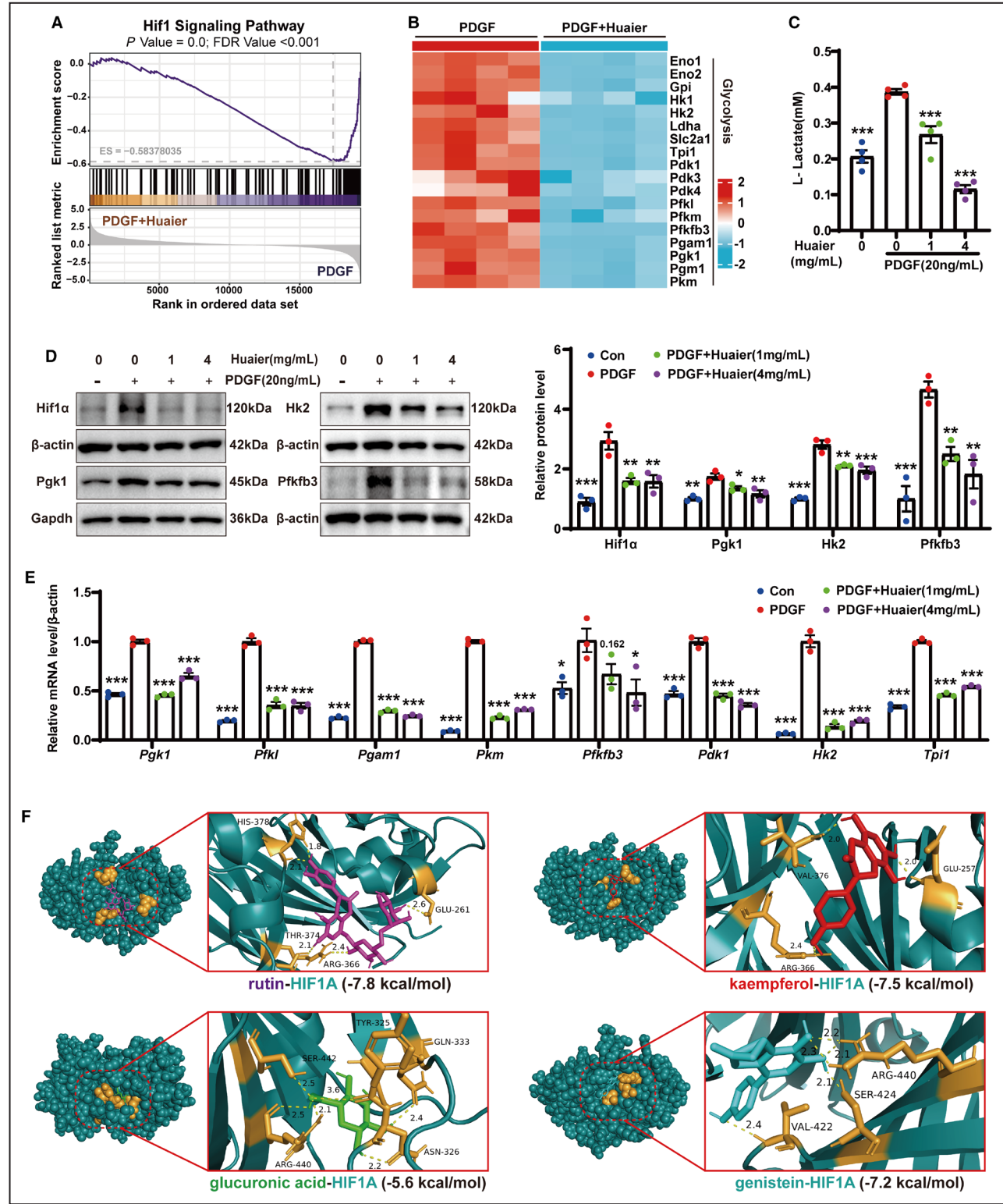
Figure 4. Effect of Huaier extract on proliferation, migration, and phenotype switching of RPASMCs.

A, Cell viability of RPASMCs treated with Huaier extract was determined using the Cell Counting Kit-8 assay. **B**, Representative images of EdU (red) incorporation reflecting RPASMCs proliferation (scale bars=100 μ m), and cell migration was evaluated through wound-healing assays at 0 and 24 hours (scale bars=500 μ m). **C**, Quantification of EdU-positive cells in **(B)**. **D**, Quantification of wound closure in **(B)**. **E**, Quantitative analysis of cell cycle distribution in **(F)**. **F**, Representative images of cell cycle and apoptosis analysis by flow cytometry. **G**, Quantitative analysis of cell apoptosis in **(F)**. **H**, Western blot analysis was used to detect the protein expression levels of PcnA, Ccnd1 and P27, normalized to β -actin. For **(B)–(H)**, RPASMCs were treated with gradient concentrations of Huaier extract (0, 1, 2, 4, and 6 mg/mL) for 48 hours under PDGF stimulation (20 ng/mL). The results are representative of 3 to 5 separate experiments. The data are presented as mean \pm SE; *P* values were determined by 1-way ANOVA with Bonferroni post hoc test (**A**, **G**, and **H**) and Welch ANOVA with Tamhane T2 post hoc test (**C**, **D**). **P*<0.05, ***P*<0.01, and ****P*<0.001 vs PDGF group. Con indicates control; PDGF, platelet-derived growth factor; and RPASMCs, rat pulmonary artery smooth muscle cells.

model and mitigate pulmonary vascular remodeling by inhibiting STAT3 (signal transducer and activator of transcription 3)/HIF-1 α /VEGF (vascular endothelial growth factor) and FAK (focal adhesion kinase)/AKT signaling pathways.²⁸ Luo et al. demonstrated that Coptidis Rhizoma effectively inhibits the proliferation of PSMCs and pulmonary vascular remodeling in experimental PH models by suppressing the expression of MAPK1 (mitogen-activated protein kinase 1), NOX4 (NADPH oxidase 4), and CYP1B1.²⁹ Similarly, Chen et al. reported that resveratrol confers protection against PH by modulating nitric oxide (NO) metabolism, inflammatory responses, and PSMCs proliferation.³⁰ Song et al. indicated that luteolin significantly reverses pulmonary vascular remodeling in PH rats by inhibiting the aberrant proliferation of PSMCs, achieved through the downregulation of the protein expressions of COX1 (cyclooxygenase-1), 5-LOX (5-lipoxygenase), 12-LOX, and 15-LOX, thereby affecting the levels of metabolites in the arachidonic acid pathway.³¹ In addition, recent studies have demonstrated that genistein and curcumin could inhibit PSMCs proliferation and pulmonary vascular remodeling by regulating HIF-1 α /NOX4 pathway and AKT/GSK3 β (glycogen synthase kinase-3 beta) signaling pathway respectively.^{32,33} However, in contrast to Western medicine, which is characterized by drugs with clearly defined compositional structures, TCM encounters several challenges in the context of clinical trials. A primary challenge is the inherent complexity of TCM formulations, which typically comprise multiple herbs and compounds that interact in intricate and often synergistic ways. This complexity poses significant difficulties in establishing standardized dosages and evaluating the efficacy and safety of TCM treatments in a manner that is directly comparable to the evaluation processes used for Western pharmaceuticals. Moreover, the variability in the quality and composition of ingredients poses another challenge. Without strict quality control, the therapeutic effects seen in clinical trials can vary, complicating the assessment of TCM's effectiveness.³⁴ Fortunately, Huaier, as a new anticancer medication, has been approved by the National Medical Products Administration to be used alone or in combination with conventional therapy for the treatment of various

cancers. It is currently used in treating primary liver cancer, and large-scale clinical trials for gastric cancer, breast cancer, and other malignant tumors have shown no safety issues.⁷ Given the similarities between the pathological mechanisms of cancer and PH, such as abnormal cell proliferation and metabolic reprogramming, Huaier presents a promising candidate for PH treatment. However, its therapeutic potential in PH remains largely unexplored. Here, we demonstrated that Huaier treatment effectively reversed the pathological phenotypic switch in PSMCs, as evidenced by the suppression of hyperproliferation and the restoration of apoptotic homeostasis. Furthermore, chronic intragastric administration of Huaier in both hypoxia-induced mouse models and monocrotaline-induced rat models resulted in significant amelioration of established experimental PH. This was indicated by improved pulmonary hemodynamics, such as reduced RVSP, decreased pulmonary vascular remodeling, and enhanced RV function. Importantly, these therapeutic effects were achieved without any observable adverse effects and also seem to improve monocrotaline induced hepato- and renal toxicity, highlighting the favorable safety profile of Huaier in the management of PH.

In this study, we further demonstrated that Huaier effectively inhibits the proliferation of PSMCs by targeting multiple regulatory pathways. Mechanistically, Huaier significantly activated the Nrf2 signaling pathway while inhibiting the NF- κ B and Hif1 α signaling pathways, thereby suppressing glycolysis, oxidative stress, and inflammation, which ultimately contribute to PSMCs proliferation. The orderly progression of glycometabolism is fundamental to maintaining vascular function. However, under the influence of PH-inducing factors, intracellular metabolic reprogramming tends to shift from oxidative phosphorylation to glycolysis, a phenomenon known as the Warburg effect. This shift preferentially supports the rapid proliferation of PSMCs. Increasing evidence highlights the role of glycolysis in the pathogenesis of PH.³⁵ Animal models of PH demonstrate increased glycolytic activity, which facilitates the proliferation of PSMCs, pulmonary vascular remodeling and RVH. Hif1 α has been implicated in the promotion of glycolysis across various



cancer types through the upregulation of numerous glycolytic genes. Elevated levels of Hif1α have been detected in thickened PAs, and inhibition of Hif1α has been shown to reduce pulmonary vascular remodeling.³⁶ Importantly, we found that the treatment of Huaier was able to suppress Hif1α expression and exert antiglycolytic effects on PH-PASMCs. This was evidenced by the downregulation of glycolysis-related genes, including *Pgk1*, *Pfk1*, *Pgam1*, *Hk2*, and *Pfkfb3*, among others.

Figure 5. Huaier extract inhibits PDGF-induced glycolysis in RPASMCs by suppressing Hif1 α signaling pathway.

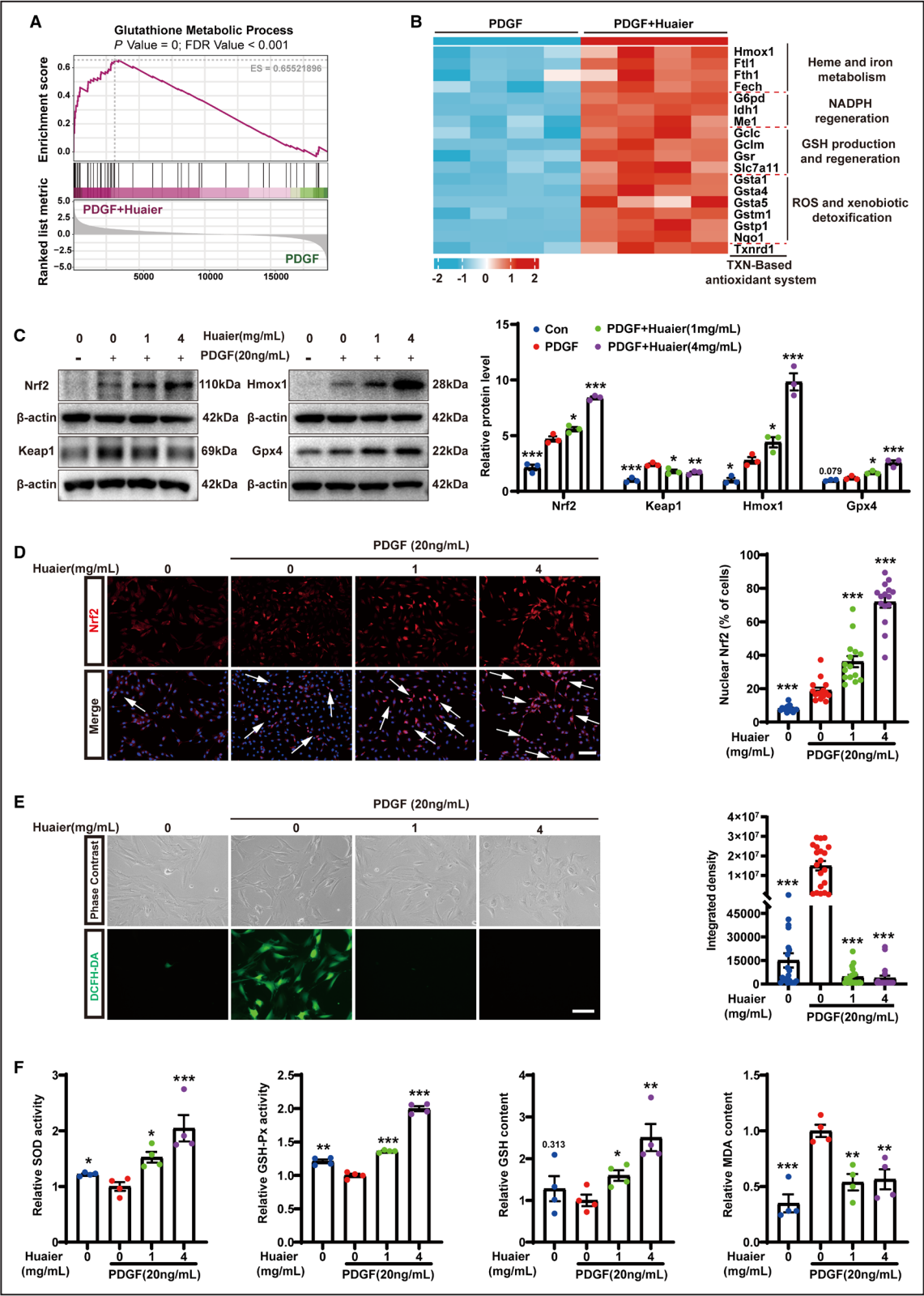
A, GSEA enrichment plots based on RNA-sequencing profiles of RPASMCs showing Huaier extract treatment result in the down-regulation of the Hif1 α signaling pathway. **B**, Clustering heatmap of glycolysis related genes in the RNA-sequencing data between PDGF and PDGF+Huaier treated RPASMCs (n=4). **C**, L-lactate levels in RPASMCs exposed to varying concentrations of Huaier extract (0, 1, and 4 mg/mL). **D**, Protein expression levels of Hif1 α , Pgk1, Hk2, and Pfkfb3 were determined by Western blot analysis. Gapdh or β -actin served as a control to confirm equal loading. **E**, Relative mRNA expression of key enzymes involved in glycolysis. **F**, Visualization of binding modes between Huaier extract related ingredients and Hif1 α by molecular docking analysis. The results are representative of 3 to 5 separate experiments. The data are presented as mean \pm SE; *P* values were determined by 1-way ANOVA with Bonferroni post hoc test (**C–E**). **P*<0.05, ***P*<0.01, and ****P*<0.001 vs PDGF group. Con indicates control; FDR, false discovery rate; GSEA, gene set enrichment analysis; Hif1 α , hypoxia-inducible factor 1-alpha; PDGF, platelet-derived growth factor; and RPASMCs, rat pulmonary artery smooth muscle cells.

Oxidative stress and inflammation have been widely implicated in the progression of PH in numerous studies.^{35,37,38} Here we demonstrated that Huaier significantly reduced cytosolic ROS in PH-PASMCs, while enhancing the nuclear translocation of Nrf2 and increasing the expression of Nrf2, Hmox1, and Gpx4. As a transcription factor, Nrf2 plays a pivotal role in maintaining redox homeostasis by regulating the expression of detoxification enzymes and antioxidant proteins, thereby safeguarding cells against oxidative and inflammatory damage. Consequently, the mechanism by which Huaier reduces cytosolic ROS likely involves the activation of Nrf2, which is vital for managing oxidative and electrophilic stress responses and results in the downregulation of NADPH oxidase activities. Moreover, the activation of Nrf2 leads to increased NO levels and decreased superoxide production.³⁹ Huaier further enhances NO production by augmenting the activity of inducible NO synthase.⁴⁰ Consequently, Huaier may exert its therapeutic effects against PH by upregulating NO production. This finding suggests that Huaier's pharmacological action against PH does not depend only on altering PASMCs phenotypes. In vitro and preclinical studies suggest that oxidative stress contributes to the development of PH and underscore the therapeutic potential of antioxidants.⁴¹ However, clinical research findings remain inconsistent.⁴² The paradoxical effects of oxidative stress in PH appear to be dependent on the disease stage. During the early phase of PH, increased oxidative stress is associated with reduced antioxidant activity, which promotes the proliferation of PASMCs and contributes to the pathogenesis of PH. Antioxidant intervention at this stage may mitigate the extent of subsequent adaptive pulmonary vascular remodeling.⁴³ In contrast, in advanced PH, hyperproliferative and apoptosis-resistant cells enhance intracellular antioxidant levels to counterbalance excessive ROS production and oxidative damage. The administration of exogenous antioxidants at this stage may inadvertently enhance adaptive antioxidant responses, thereby accelerating cell cycle progression and proliferation, and exacerbating vascular remodeling. Therefore, a comprehensive understanding of the stage-specific roles of oxidative stress is crucial for

optimizing antioxidant therapy. Given the multifactorial nature of PH pathophysiology, monotherapy targeting oxidative stress is inadequate; thus, a combinatorial therapeutic strategy is essential. Based on previous research and our current findings, we hypothesize that Huaier may influence PH and pulmonary vascular remodeling through multifaceted regulation, extending beyond simple antioxidative stress.

Furthermore, inflammatory cytokines play a crucial role in NF- κ B signaling and are essential for the proliferation of PASMCs and vascular remodeling.³⁷ Our findings indicate that Huaier treatment effectively suppresses the expression of several cytokines, including IL-1 α , IL-1 β , IL-6, TNF- α , Ccl2, Ccl5, and Ccl7, among others. This suggests that the anti-inflammatory properties of Huaier may represent a primary mechanism of its therapeutic action. The complement system significantly contributes to the development and progression of PH by perpetuating inflammation and promoting pulmonary vascular remodeling. Research has shown that complement activation, particularly involving the C3 component, plays a role in the inflammatory processes underlying PH.⁴⁴ In our study, transcriptome enrichment analysis of PAs revealed a significant decrease of components in Huaier treatment group as compared with controls, suggesting that Huaier treatment may also exert its effects through the inhibition of complement activation.

The physical alterations associated with vascular remodeling in PH encompass endothelial cell disruption in the tunica intima, hypertrophy of PASMCs in the tunica media, and fibroblast stimulation in the tunica adventitia, along with the activation of perivascular macrophages. Among these changes, the proliferation of PASMCs plays a pivotal role. In our study, both transcriptome enrichment analysis of pulmonary arteries and the analysis of the active components of Huaier indicated a regulatory effect on PASMCs proliferation and contraction. Another critical process contributing to pulmonary vascular remodeling is the epithelial-to-mesenchymal transition of endothelial cells, characterized by a complex array of biological and biochemical alterations. Huaier has been demonstrated to inhibit the epithelial-to-mesenchymal



transition process by downregulating the expression of twist and LC3 in gastric and breast cancer, respectively.⁴⁵ Importantly, our findings also suggest that

Huaier treatment can suppress the proliferation and epithelial-to-mesenchymal transition of pulmonary microvascular endothelial cells (data not shown). In

Figure 6. Huaier extract inhibits PDGF-induced oxidative stress in RPASMCs by promoting Nrf2 signaling pathway.

A, GSEA enrichment plots showing Huaier extract treatment in RPASMCs result in the upregulation of the glutathione metabolic process. **B**, Clustering heatmap of oxidative stress related genes in the RNA-sequencing data between PDGF and PDGF+Huaier treated RPASMCs (n=4). **C**, Protein expression levels of Nrf2, keap1, hmx1 and Gpx4 in RPASMCs. β -actin was used as a loading control. **D**, Representative fluorescence images depict the expression of Nrf2 (red) and DAPI (blue) across various groups, and quantification of Nrf2 nuclear translocation in RPASMCs (scale bars=100 μ m). **E**, ROS production in RPASMCs was measured by DCFH-DA fluorescent staining (scale bars=100 μ m). **F**, The content of SOD, GSH-Px, GSH and MDA in PASMCS. The results are representative of 3 to 5 separate experiments. The data are presented as mean \pm SE; *P* values were determined by 1-way ANOVA with Bonferroni post hoc test (**C** and **F**) and Welch ANOVA with Tamhane T2 post hoc test (**D**, **E** and **F** for GSH-Px). **P*<0.05, ***P*<0.01, and ****P*<0.001 vs PDGF group. Con indicates control; FDR, false discovery rate; GSEA, gene set enrichment analysis; GSH, glutathione; GSH-Px, glutathione peroxidase; MDA, malondialdehyde; NADPH, nicotinamide adenine dinucleotide phosphate; Nrf2, nuclear factor erythroid 2-related factor 2; PDGF, platelet-derived growth factor; RPASMCs, rat pulmonary artery smooth muscle cells; ROS, reactive oxygen species; and SOD, superoxide dismutase.

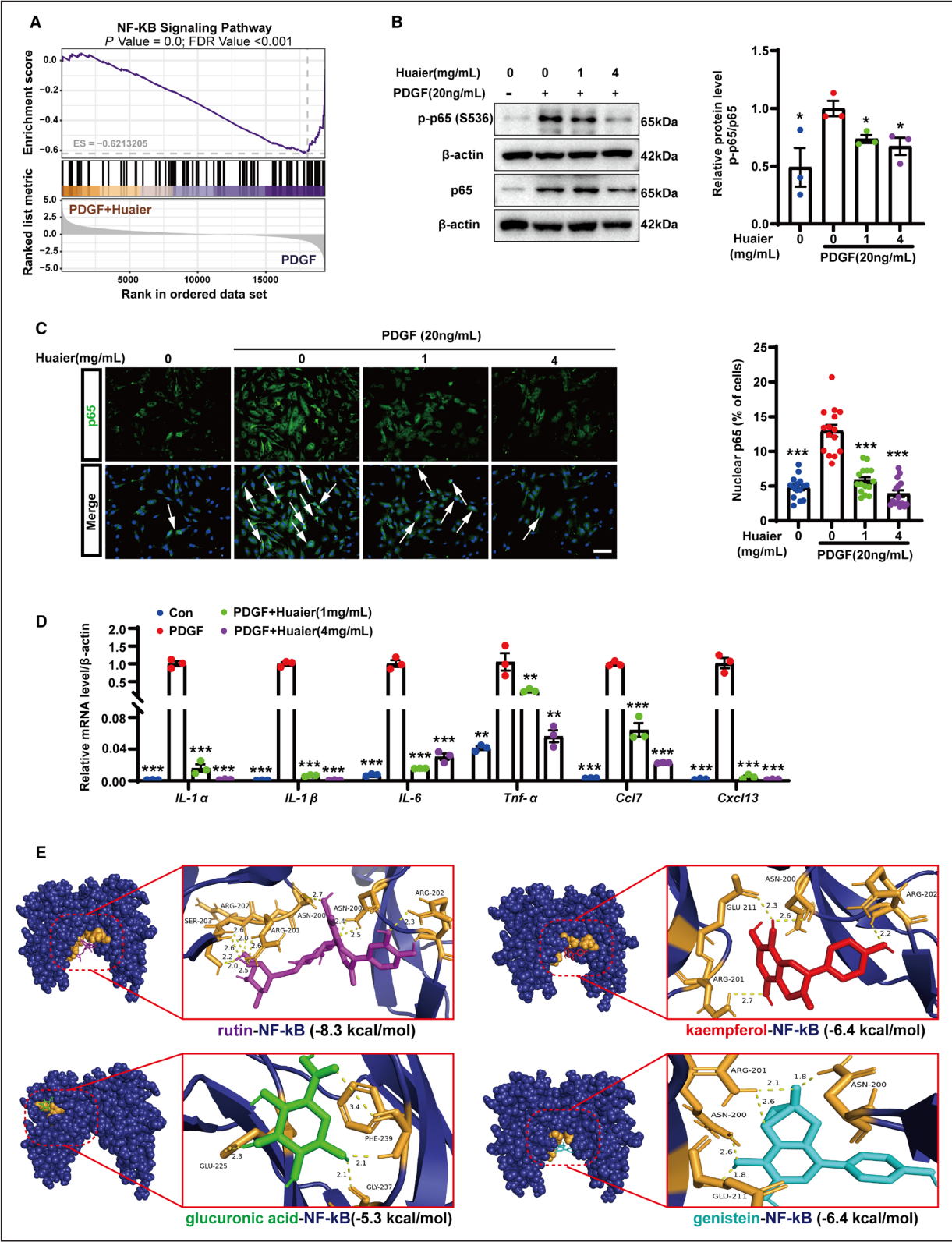
the pathogenesis of PH, dysregulation of the innate immune system can lead to immune deficiency and persistent chronic inflammation, which subsequently promotes endothelial cell dysfunction and the proliferation of PASMCS, ultimately culminating in vascular remodeling. Research has indicated that Huaier possesses the ability to modulate macrophage polarization, thereby inhibiting the polarization toward the M2 phenotype while enhancing phagocytic activity.⁴⁶ Furthermore, a recent study demonstrated that Huaier regulates cancer immunity in triple-negative breast cancer by suppressing cancer-associated fibroblasts, underscoring its critical role as an effective adjuvant agent in immunotherapy.⁴⁷ Nevertheless, the potential role of Huaier in regulating the function of fibroblasts and perivascular macrophages during the development of PH remains to be elucidated.

Numerous studies have demonstrated that Huaier can inhibit tumor cell proliferation, induce tumor cell apoptosis, and suppress tumor angiogenesis, while also exhibiting significant immunomodulatory effects. Huaier granule, recognized for its potent broad-spectrum antitumor properties, has been approved for clinical use in China. However, the elucidation and isolation of the specific bioactive components responsible for its therapeutic efficacy pose significant challenges due to its highly complex composition. To date, 4 bioactive constituents have been identified from Huaier, including rutin, kaempferol, glucuronic acid, and genistein. These compounds exhibit tumoricidal cytotoxicity and immunoregulatory properties, collectively contributing to the antitumor pharmacological effects of Huaier.⁷ The construction of a component-target network showed that 147 genes were affected by these small-molecule compounds. Molecular docking studies have demonstrated that the bioactive constituents of Huaier exhibit a strong binding affinity to target proteins, including Hif1 α and NF- κ B, among others, with binding energies <-5 kcal/mol. Despite these computational predictions, the possibility of alternative regulatory mechanisms cannot be dismissed. Notably, the activation of Nrf2 by Huaier may occur via

phosphorylation mediated by PERK/PKR (protein kinase R like kinase/protein kinase R), rather than through direct activation of Nrf2.⁴⁸ Additionally, the inhibitory effects of Huaier on the NF- κ B pathway, whether facilitated by TNF- α or other chemokine agents, necessitate further validation. Our findings also indicate a significant reduction in the expression of several cell receptor-related genes following Huaier treatment. These genes, including *Itga5*, *Notch3*, *Vcam1*, *Nlrp3*, *Cmk1r1*, and *Tlr7*, are known to be markedly upregulated in PASMCS under PH conditions. Although our current data do not directly elucidate the binding interactions between Huaier's active components and specific receptors, they lay a solid groundwork for future target discovery. Subsequent research should prioritize the isolation of bioactive monomers and use biophysical techniques, such as surface plasmon resonance, or genetic methodologies, such as knockout studies, to resolve these mechanistic ambiguities.

In this study, our findings indicate that Huaier inhibits the proliferation of PH-PASMCS in a dose-dependent manner through its antiglycolytic, anti-inflammatory, and antioxidant properties. These protective effects are likely mediated by the inhibition of the Hif1 α and NF- κ B pathways, as well as the activation of the Nrf2 signaling pathway. Consistently, Huaier treatment effectively ameliorated both hypoxia-induced PH in mice and monocrotaline-induced PH in rats. Altogether, Huaier is a potential therapeutic medicine with multitarget characteristics to prevent the progression of pulmonary vascular remodeling in rodent models of PH, suggesting its potential as a promising therapeutic agent for patients with clinical PH.

There are several limitations to our study. A primary limitation is the unresolved identification of the specific bioactive constituents in Huaier that are responsible for its antipulmonary vascular remodeling effects. However, the assessment of the whole extract aligns with traditional medicinal practices, which emphasize the synergistic effects of multiple components as the foundation for therapeutic efficacy, thereby preserving clinical relevance. Building



on our preclinical validation of Huaier's efficacy, future research should focus on bioactivity-guided fractionation to identify the specific antiremodeling compounds and elucidate their pharmacodynamic

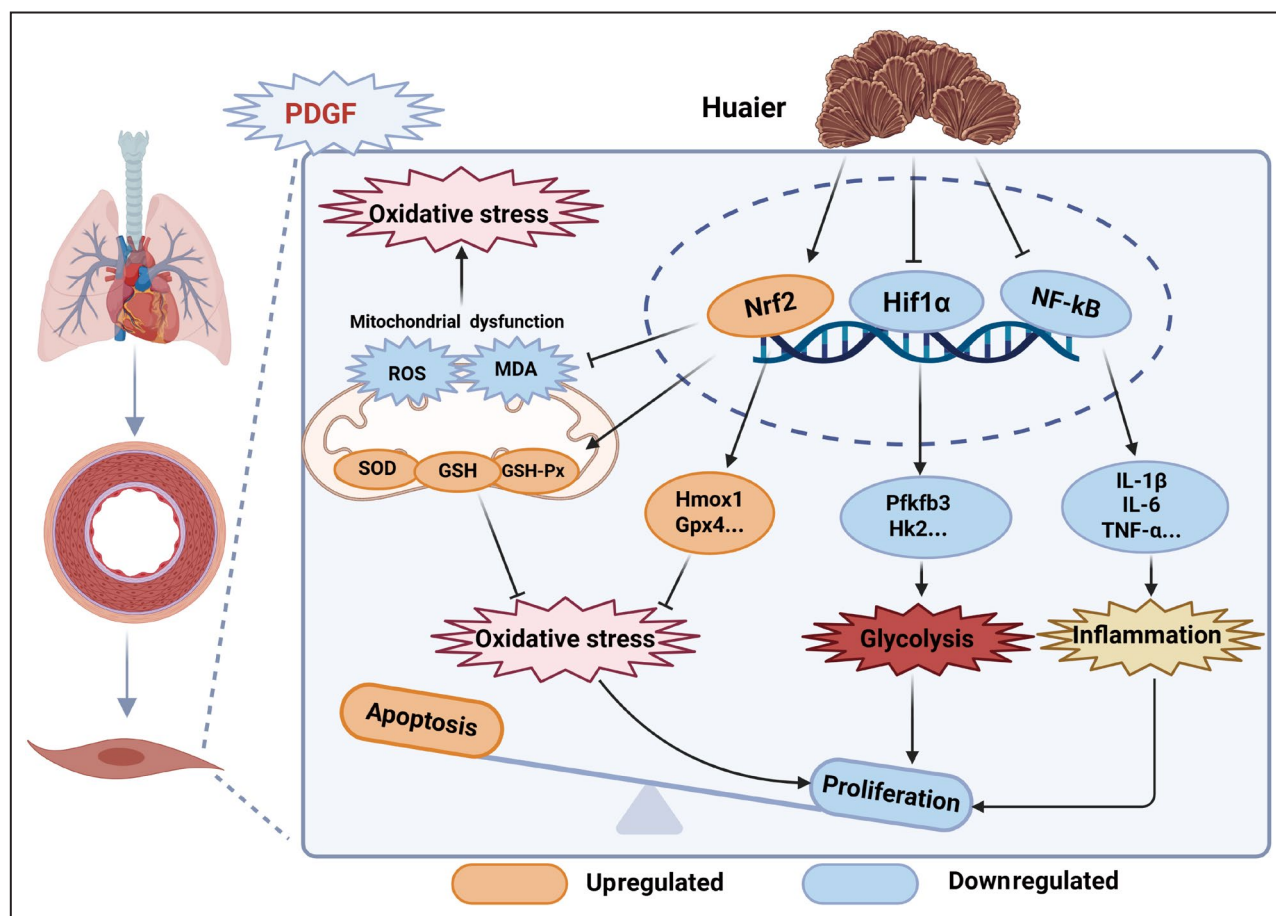
interactions. Additionally, new therapeutic strategies for PH should demonstrate incremental benefits over the optimized regimen of currently approved therapies.³⁹ Consequently, future studies could investigate

Figure 7. Huaier extract inhibits PDGF-induced activation of NF- κ B signaling pathway in RPASMCs.

A, GSEA enrichment plots based on RNA-sequencing profiles of RPASMCs showing Huaier extract treatment result in the downregulation of the NF- κ B signaling pathway. **B**, Western blot analysis of p65 and p-p65(S536), normalized to β -actin. **C**, Representative images and quantification of p65 (green) immunofluorescence staining in RPASMCs (scale bars=100 μ m). **D**, RT-qPCR was used to verify the mRNA levels of inflammation-related genes in RPASMCs. **E**, Molecular docking simulation of Huaier extract ingredients with NF- κ B. The results are representative of 3 to 5 separate experiments. The data are presented as mean \pm SE; *P* values were determined by 1-way ANOVA with Bonferroni post hoc test (**B–D**). **P*<0.05, ***P*<0.01, and ****P*<0.001 vs PDGF group. Con indicates control; FDR, false discovery rate; GSEA, gene set enrichment analysis; NF- κ B, nuclear factor κ B; PDGF, platelet-derived growth factor; RPASMCs, rat pulmonary artery smooth muscle cells; and RT-qPCR, real-time quantitative polymerase chain reaction.

the efficacy of Huaier extract in combination with other agents, such as tadalafil, to enhance treatment outcomes for PH. Moreover, it is crucial to compare the efficacy of Huaier treatment with these agents in forthcoming studies. Lastly, it is important to note that the animal studies conducted in this research used male mice, despite the fact that PH disproportionately affects women. In contemporary basic biomedical research on PH using animal models, male subjects are predominantly employed to eliminate the confounding effects of physiological cycles, hormones such as estrogen, and other potential variables that could influence the disease, as was the case in our study.

However, it is crucial to consider the role of sex and sex differences in the pathological mechanisms, disease susceptibility, prognosis, and treatment efficacy of PH. Future research should incorporate both sexes to provide a more comprehensive understanding of these factors. Although our study has demonstrated the therapeutic effects of Huaier on PH, significant advancements are necessary before it can be applied clinically. The question of whether Huaier exhibits comparable therapeutic effects in humans, as observed in animal models, remains unanswered, therefore clinical trials are imperative to resolve this uncertainty.

**Figure 8. A schematic diagram of the molecular mechanisms studied in this research.**

GSH indicates glutathione; GSH-Px, glutathione peroxidase; IL, interleukin; MDA, malondialdehyde; NF- κ B, nuclear factor κ B; PDGF, platelet-derived growth factor; ROS, reactive oxygen species; SOD, superoxide dismutase; and TNF- α , tumor necrosis factor alpha.

CONCLUSIONS

In summary, the results of this study demonstrate that Huaier extract activates the Nrf2 signaling pathway while inhibiting the NF- κ B and Hif1 α signaling pathways. This multitarget action of Huaier contributes to its protective roles against oxidative stress, glycolysis, and inflammation, collectively inhibiting the proliferation of PSMCs and thus ameliorating PH (Figure 8).

ARTICLE INFORMATION

Received January 23, 2025; accepted July 8, 2025.

Affiliations

Department of Forensic Medicine, Nanjing Medical University, Nanjing, China (H.Y., Y.Z., L.H., Y.F., T.Z., Q.M., Z.M., F.C., Y.Y., J.W.); Department of Rheumatology (H.Y., X.S., M.Z., Q.W.) and Department of Cardiology, the First Affiliated Hospital of Nanjing Medical University, Nanjing, China (Y.Z.) and Key Laboratory of Targeted Intervention of Cardiovascular Disease, Collaborative Innovation Center for Cardiovascular Disease Translational Medicine, Nanjing Medical University, Nanjing, China (L.H., F.C., J.W.).

Acknowledgments

Author contributions: Huangshu Ye, Yue Zhang, Li Hu, Yuxin Feng, Tianfan Zhu, Qi Meng, and Xiaoxuan Sun performed the experiments, collected and analyzed the data, and conducted bioinformatic analysis. Miaoja Zhang, Zhengsheng Mao, and Feng Chen provided guidance during the experiments. Huangshu Ye, Yanfang Yu, Qiang Wang, and Jie Wang designed the study and wrote the article. Feng Chen, Li Hu, and Jie Wang supervised the whole project. All authors contributed to the review and editing and approved the final article.

Sources of Funding

This research was supported by the National Natural Science Foundation of China grants (82225023, 82300069, 82200057, 82121001), the Natural Science Foundation of Jiangsu Province (BK20230304, BK20220321), the Natural Science Foundation of Jiangsu Higher Education Institutions of China (23KJB320005).

Disclosures

None.

Supplemental Material

Table S1–S2
Figures S1–S15

REFERENCES

- Hoeper MM, Humbert M, Souza R, Idrees M, Kawut SM, Sliwa-Hahnle K, Jing ZC, Gibbs JS. A global view of pulmonary hypertension. *Lancet Respir Med*. 2016;4:306–322. doi: [10.1016/S2213-2600\(15\)00543-3](https://doi.org/10.1016/S2213-2600(15)00543-3)
- Wang X, Zhu X, Huang W, Wang Z, Mei J, Ou L, Chen Y, Ma C, Zhang L. Super-enhancer-driven syndecan-4 regulates intercellular communication in hypoxic pulmonary hypertension. *J Am Heart Assoc*. 2024;13:e036757. doi: [10.1161/JAHA.124.036757](https://doi.org/10.1161/JAHA.124.036757)
- Hassoun PM. Pulmonary arterial hypertension. *N Engl J Med*. 2021;385:2361–2376. doi: [10.1056/NEJMr2000348](https://doi.org/10.1056/NEJMr2000348)
- Humbert M, Sitbon O, Guignabert C, Savale L, Boucly A, Gallant-Dewavrin M, McLaughlin V, Hoeper MM, Weatherald J. Treatment of pulmonary arterial hypertension: recent progress and a look to the future. *Lancet Res Med*. 2023;11:804–819. doi: [10.1016/S2213-2600\(23\)00264-3](https://doi.org/10.1016/S2213-2600(23)00264-3)
- Wang X, Wang Y, Yuan T, Wang H, Zeng Z, Tian L, Cui L, Guo J, Chen Y. Network pharmacology provides new insights into the mechanism of traditional Chinese medicine and natural products used to treat pulmonary hypertension. *Phytomedicine: Intern J Phytotherapy Phytopharmacol*. 2024;135:156062. doi: [10.1016/j.phymed.2024.156062](https://doi.org/10.1016/j.phymed.2024.156062)
- Long H, Wu Z. Immunoregulatory effects of Huaier (*Trametes robiniophila* Murr) and relevant clinical applications. *Front Immunol*. 2023;14:1147098. doi: [10.3389/fimmu.2023.1147098](https://doi.org/10.3389/fimmu.2023.1147098)
- Wu J, Tang G, Cheng CS, Yeerken R, Chan YT, Fu Z, Zheng YC, Feng Y, Wang N. Traditional Chinese medicine for the treatment of cancers of hepatobiliary system: from clinical evidence to drug discovery. *Mol Cancer*. 2024;23:218. doi: [10.1186/s12943-024-02136-2](https://doi.org/10.1186/s12943-024-02136-2)
- Ji H, Ma W, Zheng A, Tang D. The role and molecular mechanism of *Trametes Robiniophila* Murr (Huaier) in tumor therapy. *J Ethnopharmacol*. 2024;334:118578. doi: [10.1016/j.jep.2024.118578](https://doi.org/10.1016/j.jep.2024.118578)
- Jin H, Liu C, Liu X, Wang H, Zhang Y, Liu Y, Li J, Yu Z, Liu HX. Huaier suppresses cisplatin resistance in non-small cell lung cancer by inhibiting the JNK/JUN/IL-8 signaling pathway. *J Ethnopharmacol*. 2024;319:117270. doi: [10.1016/j.jep.2023.117270](https://doi.org/10.1016/j.jep.2023.117270)
- Xu DQ, Yuan XJ, Toyoda H, Hirayama M. Anti-tumor effect of Huaier extract against neuroblastoma cells in vitro. *Int J Med Sci*. 2021;18:1015–1023. doi: [10.7150/ijms.48219](https://doi.org/10.7150/ijms.48219)
- Zhu Z, Wang X, Zhang W, Gong M, Zhang S, Yang B, Qu B, Wu Z, Ma Q, Wang Z, et al. Huaier suppresses pancreatic cancer progression via activating cell autophagy induced ferroptosis. *Front Oncol*. 2022;12:960858. doi: [10.3389/fonc.2022.960858](https://doi.org/10.3389/fonc.2022.960858)
- Hu L, Wang J, Lin D, Shen Y, Huang H, Cao Y, Li Y, Li K, Yu Y, Yu Y, et al. Mesenchymal stem cell-derived nanovesicles as a credible agent for therapy of pulmonary hypertension. *Am J Respiratory Cell Molecular Biol*. 2022;67:61–75. doi: [10.1165/rcmb.2021-0415OC](https://doi.org/10.1165/rcmb.2021-0415OC)
- Hu L, Yu Y, Shen Y, Huang H, Lin D, Wang K, Yu Y, Li K, Cao Y, Wang Q, et al. Ythdf2 promotes pulmonary hypertension by suppressing Hmox1-dependent anti-inflammatory and antioxidant function in alveolar macrophages. *Redox Biol*. 2023;61:102638. doi: [10.1016/j.redox.2023.102638](https://doi.org/10.1016/j.redox.2023.102638)
- Peng G, Xu J, Liu R, Fu Z, Li S, Hong W, Chen J, Li B, Ran P. Isolation, culture and identification of pulmonary arterial smooth muscle cells from rat distal pulmonary arteries. *Cytotechnology*. 2017;69:831–840. doi: [10.1007/s10616-017-0081-8](https://doi.org/10.1007/s10616-017-0081-8)
- Bonnet S, Provencher S, Guignabert C, Perros F, Boucherrat O, Schermuly RT, Hassoun PM, Rabinovitch M, Nicolls MR, Humbert M. Translating research into improved patient care in pulmonary arterial hypertension. *Am J Respiratory Critical Care Med*. 2017;195:583–595. doi: [10.1164/rccm.201607-1515PP](https://doi.org/10.1164/rccm.201607-1515PP)
- Hu L, Wang J, Huang H, Yu Y, Ding J, Yu Y, Li K, Wei D, Ye Q, Wang F, et al. YTHDF1 regulates pulmonary hypertension through translational control of MAGED1. *Am J Respiratory Critical Care Med*. 2021;203:1158–1172. doi: [10.1164/rccm.202009-3419OC](https://doi.org/10.1164/rccm.202009-3419OC)
- Hu Y, Chi L, Kuebler WM, Goldenberg NM. Perivascular inflammation in pulmonary arterial hypertension. *Cells*. 2020;9:9. doi: [10.3390/cells9112338](https://doi.org/10.3390/cells9112338)
- Rabinovitch M, Guignabert C, Humbert M, Nicolls MR. Inflammation and immunity in the pathogenesis of pulmonary arterial hypertension. *Circul Res*. 2014;115:165–175. doi: [10.1161/CIRCRESAHA.113.301141](https://doi.org/10.1161/CIRCRESAHA.113.301141)
- Stacher E, Graham BB, Hunt JM, Gandjeva A, Groshong SD, McLaughlin VV, Jessup M, Grizzle WE, Aldred MA, Cool CD, et al. Modern age pathology of pulmonary arterial hypertension. *Am J Respir Crit Care Med*. 2012;186:261–272. doi: [10.1164/rccm.201201-0164OC](https://doi.org/10.1164/rccm.201201-0164OC)
- Kazmierczak F, Vogel NT, Prisco SZ, Patterson MT, Annis J, Moon RT, Hartweck LM, Mendelson JB, Kim M, Calixto Mancipe N, et al. Ferroptosis-mediated inflammation promotes pulmonary hypertension. *Circul Res*. 2024;135:1067–1083. doi: [10.1161/CIRCRESAHA.123.324138](https://doi.org/10.1161/CIRCRESAHA.123.324138)
- Zhao Y, Lv W, Piao H, Chu X, Wang H. Role of platelet-derived growth factor-BB (PDGF-BB) in human pulmonary artery smooth muscle cell proliferation. *J Receptor Signal Transd Res*. 2014;34:254–260. doi: [10.3109/10799893.2014.908915](https://doi.org/10.3109/10799893.2014.908915)
- Liao Y, Luo Z, Lin Y, Chen H, Chen T, Xu L, Orgurek S, Berry K, Dzieciatkowska M, Reis JA, et al. PRMT3 drives glioblastoma progression by enhancing HIF1A and glycolytic metabolism. *Cell Death Dis*. 2022;13:943. doi: [10.1038/s41419-022-05389-1](https://doi.org/10.1038/s41419-022-05389-1)
- Weise-Cross L, Resta TC, Jernigan NL. Redox regulation of ion channels and receptors in pulmonary hypertension. *Antioxidants Redox Signal*. 2019;31:898–915. doi: [10.1089/ars.2018.7699](https://doi.org/10.1089/ars.2018.7699)
- Sun HJ, Zhao MX, Ren XS, Liu TY, Chen Q, Li YH, Kang YM, Wang JJ, Zhu GQ. Salusin-beta promotes vascular smooth muscle cell migration and intimal hyperplasia after vascular injury via ROS/NF κ B/MMP-9 pathway. *Antioxidants Redox Signal*. 2016;24:1045–1057. doi: [10.1089/ars.2015.6475](https://doi.org/10.1089/ars.2015.6475)

25. Xi G, Shen X, Wai C, Vilas CK, Clemmons DR. Hyperglycemia stimulates p62/PKCzeta interaction, which mediates NF-kappaB activation, increased Nox4 expression, and inflammatory cytokine activation in vascular smooth muscle. *FASEB J*. 2015;29:4772–4782. doi: [10.1096/fj.15-275453](#)
26. Sharma S, Aldred MA. DNA damage and repair in pulmonary arterial hypertension. *Gen*. 2020;11:11. doi: [10.3390/genes1101224](#)
27. Meloche J, Pflieger A, Vaillancourt M, Paulin R, Potus F, Zervopoulos S, Graydon C, Courboulon A, Breuils-Bonnet S, Tremblay E, et al. Role for DNA damage signaling in pulmonary arterial hypertension. *Circulation*. 2014;129:786–797. doi: [10.1161/CIRCULATIONAHA.113.006167](#)
28. Wang RR, Yuan TY, Chen D, Chen YC, Sun SC, Wang SB, Kong LL, Fang LH, Du GH. Dan-Shen-yin granules prevent hypoxia-induced pulmonary hypertension via STAT3/HIF-1alpha/VEGF and FAK/AKT signaling pathways. *Front Pharmacol*. 2022;13:844400. doi: [10.3389/fphar.2022.844400](#)
29. Luo S, Kan J, Zhang J, Ye P, Wang D, Jiang X, Li M, Zhu L, Gu Y. Bioactive compounds from Coptidis Rhizoma alleviate pulmonary arterial hypertension by inhibiting pulmonary artery smooth muscle cells' proliferation and migration. *J Cardiovasc Pharmacol*. 2021;78:253–262. doi: [10.1097/FJC.0000000000001068](#)
30. Chen Y, Yuan T, Chen D, Liu S, Guo J, Fang L, Du G. Systematic analysis of molecular mechanism of resveratrol for treating pulmonary hypertension based on network pharmacology technology. *Eur J Pharmacol*. 2020;888:173466. doi: [10.1016/j.ejphar.2020.173466](#)
31. Song K, Duan Q, Ren J, Yi J, Yu H, Che H, Yang C, Wang X, Li Q. Targeted metabolomics combined with network pharmacology to reveal the protective role of luteolin in pulmonary arterial hypertension. *Food Funct*. 2022;13:10695–10709. doi: [10.1039/d2fo01424f](#)
32. Cui L, Zeng Z, Wang X, Yuan T, Wang C, Liu D, Guo J, Chen Y. Deciphering the mechanism of wogonin, a natural flavonoid, on the proliferation of pulmonary arterial smooth muscle cells by integrating network pharmacology and in vitro validation. *Curr Issues Molec Biol*. 2023;45:555–570. doi: [10.3390/cimb45010037](#)
33. Nie X, Wu Z, Shang J, Zhu L, Liu Y, Qi Y. Curcumin suppresses endothelial-to-mesenchymal transition via inhibiting the AKT/GSK3beta signaling pathway and alleviates pulmonary arterial hypertension in rats. *Eur J Pharmacol*. 2023;943:175546. doi: [10.1016/j.ejphar.2023.175546](#)
34. Xu F, Zhang H, Chen J, Zhan J, Liu P, Liu W, Qi S, Mu Y. Recent progress on the application of compound formulas of traditional Chinese medicine in clinical trials and basic research in vivo for chronic liver disease. *J Ethnopharmacol*. 2024;321:117514. doi: [10.1016/j.jep.2023.117514](#)
35. Grobs Y, Romanet C, Lemay SE, Bourgeois A, Voisine P, Theberge C, Sauvaget M, Breuils-Bonnet S, Martineau S, El Kabbout R, et al. ATP citrate lyase drives vascular remodeling in systemic and pulmonary vascular diseases through metabolic and epigenetic changes. *Sci Transl Med*. 2024;16:eado7824. doi: [10.1126/scitranslmed.ado7824](#)
36. Ball MK, Waypa GB, Mungai PT, Nielsen JM, Czech L, Dudley VJ, Beussink L, Dettman RW, Berkelhamer SK, Steinhorn RH, et al. Regulation of hypoxia-induced pulmonary hypertension by vascular smooth muscle hypoxia-inducible factor-1alpha. *Am J Respir Crit Care Med*. 2014;189:314–324. doi: [10.1164/rccm.201302-0302OC](#)
37. Hashimoto-Kataoka T, Hosen N, Sonobe T, Arita Y, Yasui T, Masaki T, Minami M, Inagaki T, Miyagawa S, Sawa Y, et al. Interleukin-6/interleukin-21 signaling axis is critical in the pathogenesis of pulmonary arterial hypertension. *Proc Natl Acad Sci USA*. 2015;112:E2677–E2686. doi: [10.1073/pnas.1424774112](#)
38. Hood KY, Montezano AC, Harvey AP, Nilsen M, MacLean MR, Touyz RM. Nicotinamide adenine dinucleotide phosphate oxidase-mediated redox signaling and vascular remodeling by 16alpha-Hydroxyestrone in human pulmonary artery cells. *Hypertension*. 2016;68:796–808. doi: [10.1161/HYPERTENSIONAHA.116.07668](#)
39. Kurosawa R, Satoh K, Kikuchi N, Kikuchi H, Saigusa D, Al-Mamun ME, Siddique MAH, Omura J, Satoh T, Sunamura S, et al. Identification of Celastramycin as a novel therapeutic agent for pulmonary arterial hypertension. *Circ Res*. 2019;125:309–327. doi: [10.1161/CIRCRESAHA.119.315229](#)
40. Yang A, Fan H, Zhao Y, Chen X, Zhu Z, Zha X, Zhao Y, Chai X, Li J, Tu P, et al. An immune-stimulating proteoglycan from the medicinal mushroom Huaier up-regulates NF-κB and MAPK signaling via toll-like receptor 4. *J Biol Chem*. 2019;294:2628–2641. doi: [10.1074/jbc.RA118.005477](#)
41. Pan J, Wang R, Pei Y, Wang D, Wu N, Ji Y, Tang Q, Liu L, Cheng K, Liu Q, et al. Sulforaphane alleviated vascular remodeling in hypoxic pulmonary hypertension via inhibiting inflammation and oxidative stress. *J Nutri Bioche*. 2023;111:109182. doi: [10.1016/j.jnutbio.2022.109182](#)
42. Poyatos P, Gratacos M, Samuel K, Orriols R, Tura-Ceide O. Oxidative stress and antioxidant therapy in pulmonary hypertension. *Antioxidants*. 2023;12:12. doi: [10.3390/antiox12051006](#)
43. Hoshikawa Y, Ono S, Suzuki S, Tanita T, Chida M, Song C, Noda M, Tabata T, Voelkel NF, Fujimura S. Generation of oxidative stress contributes to the development of pulmonary hypertension induced by hypoxia. *J Appl Physiol*. 2001;90:1299–1306. doi: [10.1152/jappl.2001.90.4.1299](#)
44. DeVaughn H, Rich HE, Shadid A, Vaidya PK, Doursout MF, Shivshankar P. Complement immune system in pulmonary hypertension-cooperating roles of circadian rhythmicity in complement-mediated vascular pathology. *Intern J Molecular Sci*. 2024;25:25. doi: [10.3390/ijms252312823](#)
45. Xu Z, Zheng G, Wang Y, Zhang C, Yu J, Teng F, Lv H, Cheng X. Aqueous Huaier extract suppresses gastric cancer metastasis and epithelial to mesenchymal transition by targeting twist. *J Cancer*. 2017;8:3876–3886. doi: [10.7150/jca.20380](#)
46. Li Y, Qi W, Song X, Lv S, Zhang H, Yang Q. Huaier extract suppresses breast cancer via regulating tumor-associated macrophages. *Sci Rep*. 2016;6:20049. doi: [10.1038/srep20049](#)
47. Li C, Wang X, Xing L, Chen T, Li W, Li X, Wang Y, Yang C, Yang Q. Huaier-induced suppression of cancer-associated fibroblasts confers immunotherapeutic sensitivity in triple-negative breast cancer. *Phytomedicine: Intern J Phytotherapy Phytopharmacol*. 2024;135:156051. doi: [10.1016/j.phymed.2024.156051](#)
48. Cullinan SB, Zhang D, Hannink M, Arvisais E, Kaufman RJ, Diehl JA. Nrf2 is a direct PERK substrate and effector of PERK-dependent cell survival. *Mol Cell Biol*. 2003;23:7198–7209. doi: [10.1128/MCB.23.20.7198-7209.2003](#)